

The Myelin Membrane of the Central Nervous System— Essential Macromolecular Structure and Function

By Wilhelm Stoffel

The neural sheaths that surround the nerve fibers (axons) are composed of myelin-specific complex lipids and are assembled during the myelination phase either by the oligodendrocytes in the central nervous system (CNS) or by the Schwann cells in the peripheral nervous system. These multilayered myelin membranes insulate the axons and permit a rapid, saltatory conduction of excitation and a reduced axon diameter in comparison with noninsulated axons. Myelination was hence the decisive evolutionary event in miniaturization of the central nervous system (brain and spinal cord). The morphology of the myelin membrane has been studied in detail mainly by electron microscopy. Most of its biochemistry has been elucidated in recent years by molecular-level analysis of both the lipid components (cholesterol, phospholipids and sphingolipids) and the constituent proteins. The multilamellar system is distinguished by a characteristic periodicity due to the 5-nm-thick bilayer formed by the myelin-specific lipids. The bilayer interacts with the myelin basic protein (MBP) on the cytosolic side of the plasma membrane process, while the integral membrane protein proteolipid protein (PLP) has hydrophilic domains exposed on both the cytosolic and extracytosolic faces of the bilayer. Numerous protein-chemical and -immunotoxicochemical findings have been summarized in a model of the myelin membrane. Through molecular biological studies, the genetic structure and chromosomal location of the myelin proteins have been determined. By employing techniques of molecular and cell biology together, it is now possible to analyze the process of myelinogenesis, the time- and location-specific expression of myelin-specific genes in the brain. Gene-technological methods have been used to define the mutations in the models jimpy mouse and myelin-deficient rat. These are animal models that correspond to genetically determined myelin defects (dysmyelinoses) in humans. Using them, it will be possible to study the cell death of oligodendrocytes on a molecular level; this process is the result of expression of mutant myelin proteins and is incompatible with life. Oligodendrocytes and the myelin structures they synthesize are the target structures of cytotoxic lymphocytes (T_c). In the course of the demyelination process in multiple sclerosis, these cause the breakdown of the myelin sheaths, in gradually appearing inflammations. T_c lymphocytes recognize myelin structures as epitopes and destroy them. The picture of the myelin membrane's molecular composition, which we are now perfecting, will also lead to a better understanding of demyelination on a molecular level, and hence to new therapeutic possibilities.

1. Introduction

In the course of evolution, organisms steadily increased in complexity, and a series of mechanisms arose which allowed them to act and react promptly to external influences. The central and peripheral nervous systems (CNS and PNS) were of great importance here, since they allowed information to be transmitted at high speed between the nerve cells (neurons) and the target organs via the nerve fibers (axons). In addition to the neurons, the neuroglia also developed; these form supportive tissue for the neurons and include the astroglia and the oligodendrocytes. The development of an electrical insulation system for the neural fibers, in the form of a myelin sheath constructed by the oligodendrocytes, was a decisive step in evolution. For naked axons, the speed of excitation transmission is proportional to the diameter of the axon. In a myelinated axon transmission occurs up to 100

times faster than in the absence of myelin; the diameter of the axon can hence be significantly decreased, while maintaining the same performance. Apart from the increase in pulse transmission speed, myelination makes room for a far greater number of axons, which makes possible the exceedingly compact structure of the CNS. If the axons of the spinal cord were not myelinated, then in order to achieve the same results the spinal cord would need to have the diameter of an oak tree several hundred years old, and the optic nerve would require a diameter not of 2–4 mm, but of 10–15 cm.

The fatty covering of the CNS axons, which is particularly obvious in the white matter of a brain section (Fig. 1), was first described by *Virchow* in 1854^[1] and named myelin (Greek *myelos*, marrow). In 1871, under the light microscope, *Ranvier*^[2] observed breaks in the myelin sheath at intervals of 1–2 μm , which today are called the nodes of Ranvier. Here, the axons are bare and carry higher concentrations of the $\text{K}^{\oplus}/\text{Na}^{\oplus}$ pumps needed to restore the action potential. The high speed of excitation transmission is not achieved by continual depolarization, as in naked axons, but in jumps from one node to the next over the internodal region. This is known as saltatory excitation.^[3] Since depolar-

[*] Prof. Dr. Dr. W. Stoffel
Institut für Biochemie
Medizinische Fakultät der Universität
Joseph-Stelzmann-Strasse 52, D-5000 Köln 41 (FRG)

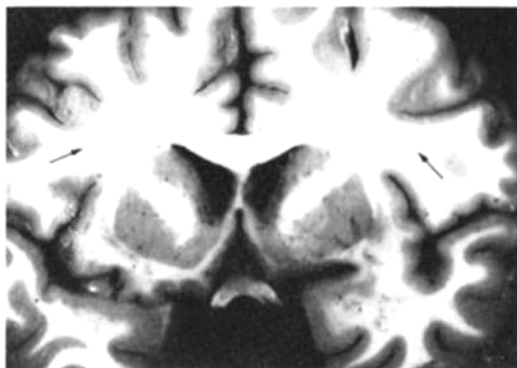


Fig. 1. Macroscopic section through the human brain. The cortex and the white matter (arrows) can be clearly seen.

ization only occurs locally, at the nodes, considerable energy is saved in repolarization.

2. Myelination

Myelin-like neural sheaths first appeared in the evolutionary step that led to the vertebrates (bony fish).^[4] The formation of myelin sheaths around the axon gave three advantages; faster information flow, compact organization of the CNS, and energy savings in restoration and maintenance of the resting potential.

Myelination (myelogenesis) takes place in the CNS in a strictly programmed manner, both in when and where it occurs. The program is begun at a characteristic point in time for each species by the precursor cells to O2A astrocytes, which differentiate into oligodendrocytes. In mice and rats this occurs about ten days after birth, in humans at the sixth month of pregnancy. Development of the myelin sheath around the neural fibers of the brain and spinal cord is largely completed in rats and mice by the thirtieth day after birth and in humans by the end of the second to fourth year.^[5] During this phase, the oligodendrocyte synthesizes two to three times its own weight in myelin components, lipids and proteins, daily.^[6] The oligodendrocytes of the CNS form extended processes of their plasma membranes (Fig. 2A), which approach up to 50 axons and wrap themselves spirally around them. In this process, the cytoplasm is almost entirely squeezed out of the membrane processes. The

interior (cytoplasmic) faces lie closely pressed together and appear under the electron microscope as the “main dense line” (MDL), because of their high electron density. In the course of wrapping around the axon, the exterior surfaces of these plasma membrane processes (extracytosolic face) also come into close contact with each other. The contact zone appears as the “intra-period dense line” (IDL). Figure 2A shows schematically the development of the myelin membrane from the plasma membrane of the oligodendrocytes, Figure 2B the spiral wrapping process, and Figure 2C the

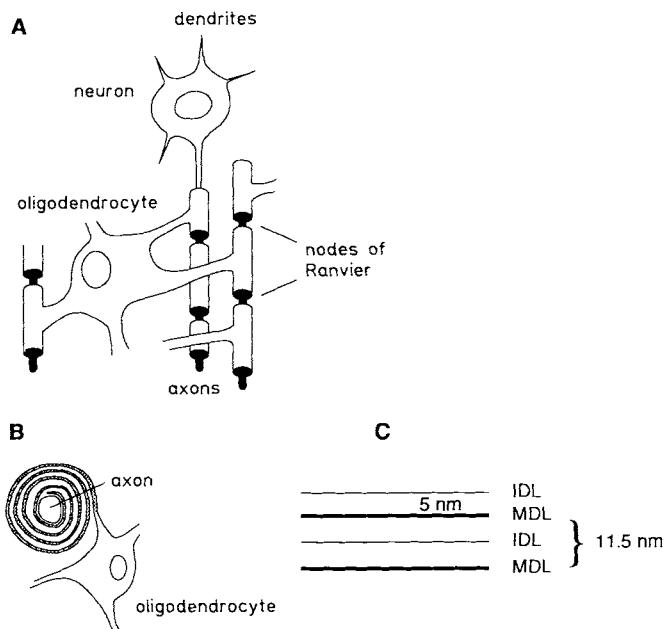


Fig. 2. A) Schematic diagram of plasma membrane processes extending from one oligodendrocyte to many axons, with formation of the nodes of Ranvier. B) Schematic diagram of the spiral winding process in myelination. C) Schematic diagram of myelin periodicity observed under the electron microscope. (see also Fig. 3).

periodicity of the myelin membrane, as seen in the electron microscopic image of a myelinated axon (section in Fig. 3).

The myelin membrane displays a periodicity of 11.5 nm. Each lipid bilayer is about 4–5 nm thick (Fig. 2C) and is therefore significantly larger than the plasma membrane of liver or connective tissue cells (2.5–3 nm). These large di-



Wilhelm Stoffel studied medicine from 1947 to 1952 in Cologne and obtained his doctorate with E. Klenk in physiological chemistry in Cologne. He studied chemistry in Bonn from 1952 to 1957 and received his Diplom with B. Helferich and his doctorate with L. Craig, Rockefeller University, New York, and E. Klenk, Cologne. After postdoctoral study with L. Craig and E. H. Ahrens, Rockefeller University, and C. Martius, ETH Zürich, he habilitated in physiological chemistry in Cologne in 1962 and took up the Chair of Physiological Chemistry in 1967 (now Biochemistry, Medical Faculty of Cologne University). His current research interests include neurochemistry and molecular neurobiology, analysis of atherogenesis (arteriosclerosis research), and structure and function analysis of serum lipoproteins.



Fig. 3. Electron microscopic image of a section through a myelinated axon. The electron-dense main dense line (MDL), corresponding to the cytosolic cleft, can be distinguished, as can the intraperiod dense line (IDL), which results from the extracytoplasmic sides of two myelin membranes packed together. The radial components are also visible.

mensions are the direct result of the various chemical structures of the lipids that form the bilayer, which will be described in the next section.

In the peripheral nervous system, the role of the oligodendrocyte in the CNS is filled by the Schwann cell. Although the PNS myelin is very similar to that of the CNS in its morphological architecture (periodicity), each Schwann cell forms only one internodal sheath.

In the following, four questions concerning the biochemistry and molecular biology of the macromolecular components of the myelin membrane of the central nervous system will be discussed:

1. Which chemical structures are responsible for the compact layering of the myelin lamellae and hence for the insulating effect on the axon, and how is the extraordinary periodicity of the myelin membrane determined?
2. How can the winding of oligodendrocyte plasma membrane processes around the axons be understood?
3. How do the slightest changes in protein structures through mutations lead to complete dysfunction and death?
4. What significance does a knowledge of myelin structures have for the understanding of pathogenic dys- and demyelinating diseases?

3. The Lipid Bilayer of the Myelin Membrane

Myelin may be isolated in homogeneous form for analysis by simple centrifugation steps. The myelin membrane is the most lipid-rich in any animal tissue. About 80% of its dry weight consists of cholesterol and complex sphingo- and phospholipids and only 20% is protein. Table 1 shows the components of myelin, compared with those of the plasma membrane of oligodendrocytes. The lipid bilayer has a very unusual composition in that it has an extraordinarily high cholesterol content of 40 mol%. Hence, for every phospholipid, one molecule of cholesterol is present (sphingomyelin is included with the phospholipids here because it has an identical zwitterionic head group to the phosphatidylcholines); relative to the sphingolipids cerebroside and sulfatide, the proportion is 1:2.

Complete extraction of the myelin lipids from the myelin is only possible with acidic chloroform/methanol (e.g., chlo-

Table 1. Comparison of the components of oligodendrocyte plasma membranes with those of myelin.

Components	Oligodendrocyte plasma membrane [mol %]	Myelin [mol %]
Proteins	54	21
Lipids	46	79
Cholesterol	36.4	40.9
Cerebrosides	9.4	15.7
Sulfatides	3.0	4.0
Sphingomyelin	5.4	4.7
Phosphatidylcholine	25.4	10.9
Phosphatidylethanolamine	7.3	13.6
Phosphatidylinositol (di)phosphate	7.1	4.7
Phosphatidylserine	5.1	5.0
Gangliosides	0.9	0.5

reform-methanol-acetic acid, 2:1:0.1), since the acidic phospholipids and sulfatides form strong ionic bonds to the myelin proteins. The amphiphilic complex lipids are made up of a hydrophobic group—the alkane chains of the fatty acids and of sphingosine, the alkenyl ethers of plasmalogens—which forms the central or core region of the bilayer, and the polar head group, which makes up the surface and faces the aqueous myelin (Figs. 4 and 5).

The hydrophobic portions of sphingolipids (cerebroside and sulfatide) are made up of extremely long fatty acids, from C₁₈ (stearic acid) to C₂₄ (lignoceric acid). These are present in their saturated, α -D-hydroxy or unsaturated ω -9-monoene forms and are bound to the sphingosine (sphingene, (2*S*,3*R*,4*E*)-2-amino-1,3-dihydroxyoctadecene) by an amide linkage to give the ceramide. The alkane chains of the fatty acid and sphingosine base portions of the ceramide are hence variable in length. The all-*trans* structure of the long-chain acyl residues (>C₂₄) dictates a length of 3.6–4.0 nm. This explains the unusual thickness of the bilayer, 4.5–5.0 nm; the “sticky ends” of the alkane chains overlap in the fluid center of the bilayer.

On the edge of the hydrophilic head group one finds the free hydroxy groups of the sphingosine and of the long-chain α -hydroxy fatty acids. Like the hydroxy group of cholesterol and the amide group of the ceramide, these can undergo hydrogen bonding to the carbonyl groups of the phospho- and sphingolipids. Hydrogen bonds reduce the distance between the groups that form them. The number of free protons available for hydrogen-bond formation allows a cross-linking of all the carbonyl groups in the lipid bilayer and, consequently, its stabilization by a two-dimensional layer of hydrogen bonds (Fig. 4). The acyl groups of the ceramides—sphingomyelin only contains long-chain, saturated, C₁₈ and C₂₄ fatty acids—would exist in crystalline form at 37 °C, but are converted into a fluid phase by intercalation of cholesterol molecules and of the acyl groups of the phospholipids, which are in part highly unsaturated. Though their function is unknown, the 1-alkenyl ether groups in the phosphatidylethanolamine class are also worth mentioning here.

Regarding the polar head groups of myelin membrane lipids at the water interphase, one finds not only the ubiquitous membrane phospholipids phosphatidylcholine and phosphatidylethanolamine, but also extensive amounts of phosphatidylserine and phosphatidylinositol. Together with

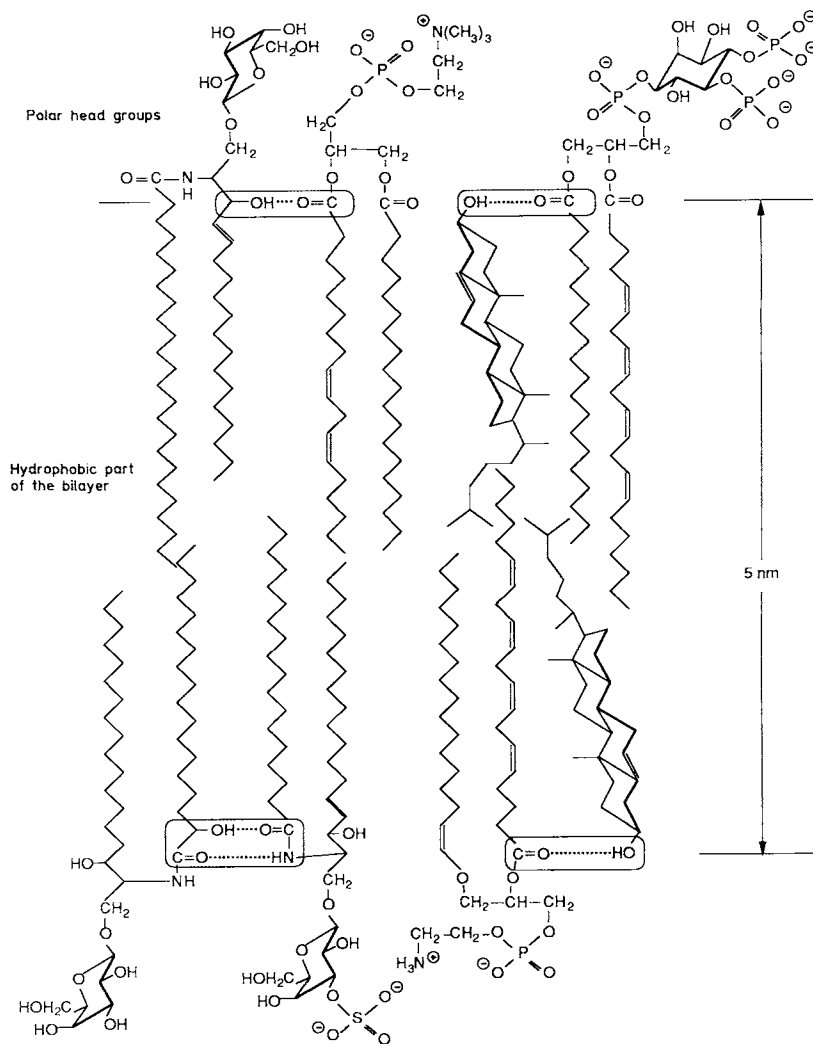


Fig. 4. Diagram of a model lipid bilayer, with cholesterol, the myelin-specific sphingolipids cerebroside and sulfatide, and the acidic phospholipids. The four possible types of hydrogen bonding are emphasized. The chemical structures of myelin lipid species are presented in more detail in Figure 5.

the sulfatides, this means that on average every fourth polar head group of the complex phospho- or sphingolipid type contributes an anionic group to the membrane surface. The gangliosides, which are present as trace lipids in myelin membranes, too, have not been included here (Fig. 5).

At present we know little about the symmetry or asymmetry of lipid distribution in the bilayer. Labeling of the oligodendrocyte plasma membrane and the myelin membrane with anti-galactosylceramide or anti-sulfatide antibodies, however, reveals their dense distribution in the external layers of the membrane sandwich structure.

Because of the zwitterionic head groups of the phospholipids, the hydrophilic, uncharged galactose residues of the cerebroside, and above all the anionic groups, the surfaces of the myelin membrane bilayer have many and varied possibilities for interaction with complementary molecules on both the cytosolic and extracytoplasmic faces of the membrane. These may well be important for compact packing and for the spiral folding process in myelination.

The significance of the relatively high content of phosphatidylinositols, especially with regard to their importance as a "second messenger system", is quite unknown.

4. Myelin Proteins of the CNS

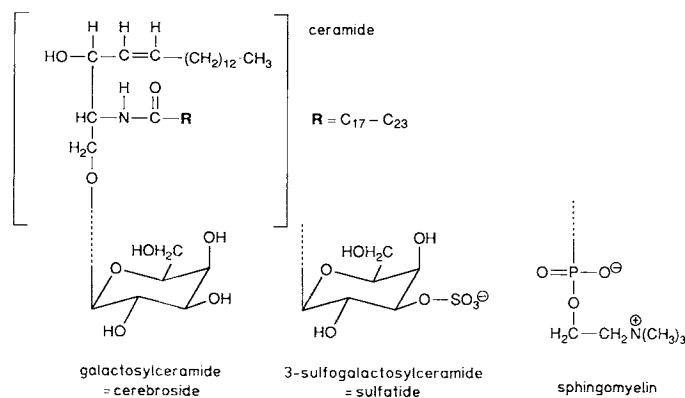
Although the myelin lipids of the PNS and CNS are very similar in composition, significant differences are found for the proteins. Sodium dodecyl sulfate polyacrylamide gel electrophoresis (SDS-PAGE) separates the myelin protein mixture into a few components (Fig. 6).

The bands can be assigned to proteolipid protein (PLP), also called lipophilin, to DM 20, an isoprotein derived from PLP, and to the myelin basic protein (MBP) and its isoforms. The latter are lower-molecular-weight forms of MBP, which arise by alternative splicing (see Section 5, Fig. 8). The remaining bands correspond to glycoproteins, Wolfgram proteins (W), and myelin-associated glycoproteins (MAG). Together, PLP and MBP make up about 90% of the total protein.

4.1. Myelin Basic Protein

Myelin basic proteins constitute some 30–40% of the total protein in myelin and can be purified by acid extraction

Sphingolipids



Phospholipids

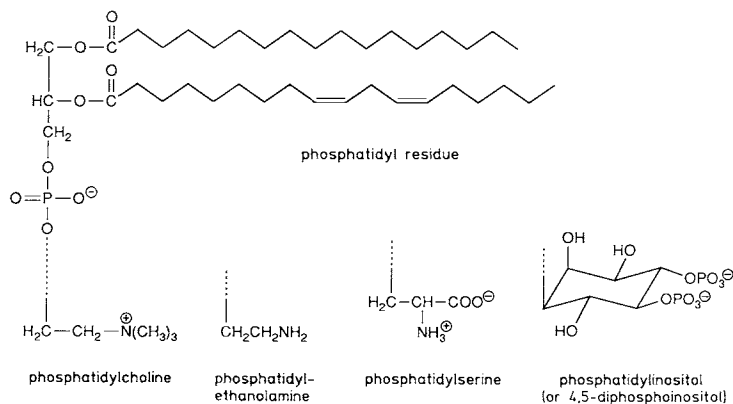


Fig. 5. Structural formulas of the most important classes of lipid in the myelin membrane.

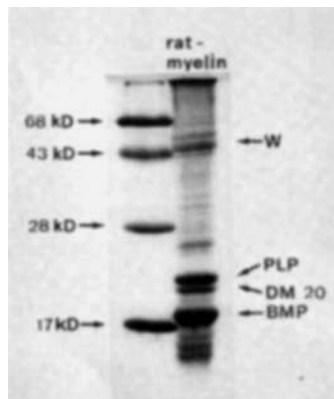


Fig. 6. Right: SDS-polyacrylamide gel electrophoresis of rat myelin proteins. Left: standards. W, Wolfgram proteins; PLP, proteolipid protein; DM 20, isoform of PLP; BMP, myelin basic protein (otherwise abbreviated MBP in this article).

of the myelin with subsequent ion-exchange chromatography and gel filtration.^[7] The main component in humans and cattle is an 18.5-kDa MBP with 169 amino acids (bovine) or 170 amino acids (human, with 24% basic amino acids).^[9] In humans there are two isoforms, 17.2 kDa and 21.5 kDa in size,^[10] while rodents have four isoforms of 14, 17, 18.5, and 21.5 kDa. Here,^[10, 11] as in humans,^[12] these

arise by alternative splicing of *one* primary transcript of the MBP gene,^[11] which will be discussed in detail with the description of the MBP gene structure (Section 5). MBP shows all the characteristics of a peripheral membrane protein. It has been localized in the cytoplasmic space (visible as the MDL under the electron microscope) with the aid of specific antibodies^[13] and by enzymatic degradation of myelin proteins.^[14] Because of its high basicity, MBP undergoes ionic interactions with the acidic polar head groups of lipids on the cytoplasmic side of the lipid bilayers, and brings about their compact packing.

In aqueous solution, circular dichroism measurements have shown that MBP occurs predominantly in a random coil conformation.^[15] Stoner,^[16] on the other hand, has proposed a secondary pleated sheet structure, on the basis of secondary-structure parameter weightings in computer calculations.

4.2. Proteolipid Proteins

The proteolipid fraction was first isolated by *Folch and Lees* in 1951 from a chloroform-methanol extract of the white matter of the brain.^[17] It is the largest protein fraction in myelin, making up 50–55% of the dry weight. SDS-PAGE separates it into two bands, of 26 kDa (PLP) and 20 kDa (DM 20). PLP and DM 20 are isoproteins, which, because of their high hydrophobicity, are water-insoluble. The principal reason why 30 years elapsed between their discovery and the elucidation of their primary structure in my group in Cologne (1982–1983) was the necessity to develop new separation methods for hydrophobic peptides. These peptides were obtained by chemical cleavage (cyanogen bromide cleavage at methionine residues and bromosuccinimide-dimethyl sulfoxide (DMSO) cleavage at tryptophan residues) and enzymic degradation of the PLP; their separation was followed by Edman degradation of the purified peptides.

We studied human and bovine brain. PLP is a polypeptide with 276 amino acids and a molecular mass of 29 891 Da. Surprisingly, we found that the sequences of human and bovine PLP differ at only two positions: Ala 188 and Thr 198 in bovine PLP are replaced by Phe 188 and Ser 198 in human PLP (Fig. 7, top). The sequence is clearly divided into one short and four long hydrophobic sequences, connected by hydrophilic “loops”. If one arranges these domains separately (Fig. 7, bottom) and calculates their three-dimensional size, the structures typical of an integral membrane protein emerge. Three domains have just the right size to span the 5-nm bilayer (*trans* helices), while two are present in *cis* configuration, since one domain (40 amino acids) is too long to span the membrane, and the other (12 amino acids) is too short. In addition, both of these contain proline residues in the center of the sequence; proline is an α -helix breaker and leads to a bend and a reversal in the direction of the α -helix. PLP contains 14 cysteine residues, four of them as free cysteines. A disulfide bond is found between Cys 227 and the amino-terminal Cys 5. The hydrophobicity of the polypeptide is increased still further by acylation with a long-chain fatty acid on Thr 198.

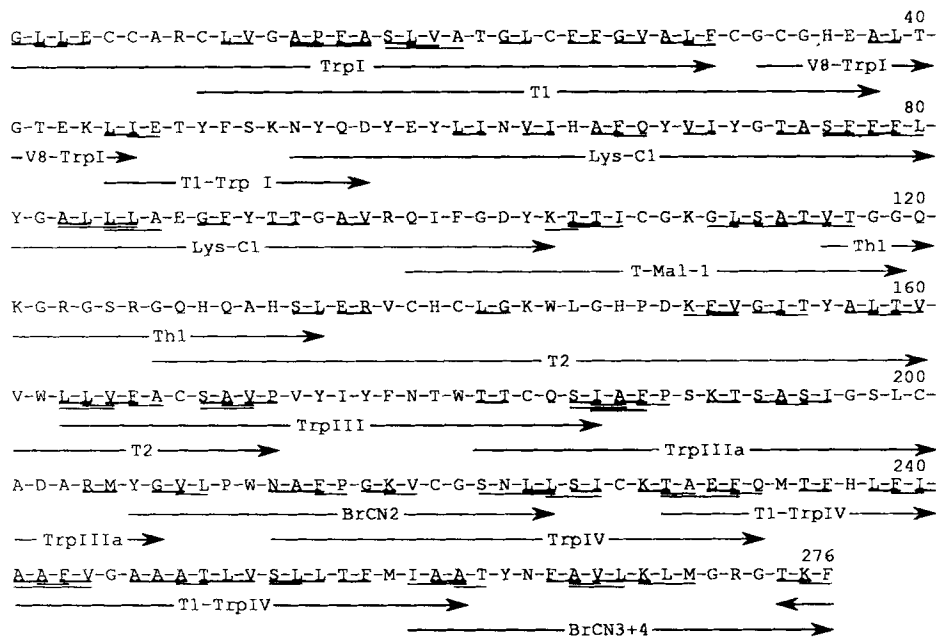
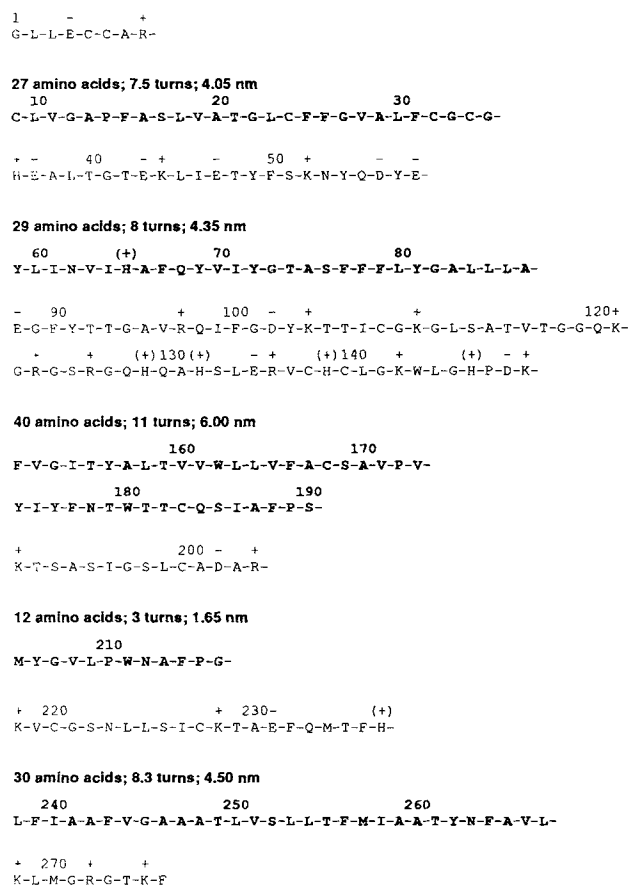


Fig. 7. Top: Amino-acid sequence and sequencing strategy for human proteolipid protein of the central nervous system. Trp, tryptophan fragments I-IV; V8, V8 staphylococcus protease; Lys-C, Lys-C protease; T-Mal, trypsin fragment after maleoylation; Th, thermolysin fragment; T, tryptic peptides; BrCN, cyanogen bromide fragments I-IV. Bottom: Hydrophobic (bold) and hydrophilic domains of the proteolipid protein. Above the sequences are the amino-acid numbers, the number of turns in the α -helix they form (3.6 amino acids per turn), and the length of the resulting helix (0.5 nm per turn).



4.2.1. Configuration of the Proteolipid Protein in the Myelin Membrane

From the strict division of the PLP polypeptide chain into hydrophobic and hydrophilic domains, a model was proposed for its integration into the myelin lipid bilayer. This was then confirmed by biochemical and immunotopochemical studies. Figure 8 (top) illustrates our current view. On the

extracytoplasmic side, one finds a short, hydrophilic, N-terminal sequence, which continues into the first transmembrane α -helix. This, in turn, leads into a hydrophilic domain with two excess negative charges on the cytoplasmic side and folds back onto itself into the second transmembrane helix. The largest, strongly positively charged, hydrophilic sequence (Arg 97 to Arg 150) is found on the extracellular surface. The two *cis* domains also dip into the membrane bilayer from this side, while the C-terminal hydrophobic domain traverses the membrane again, so that the highly positively charged C-terminus of the sequence is oriented towards the cytoplasmic space. The hydrophobic segments are bounded by anionic or cationic amino-acid side chains or by ionic side chains of zwitterionic nature.

In our model, ten cysteine residues lie in the hydrophilic domains on the extracytoplasmic surface and four are found in α -helical domains. On the basis of the disulfide bridge between Cys 5 and Cys 227, and possible disulfide linkages between the *trans* and *cis* helices, we assume a cylindrical aggregation of the hydrophobic helices, as depicted in Figure 8 (bottom). On limited proteolysis of the myelin membrane, we observe facile release of the small hydrophilic domain between Arg 204 and Lys 217 and its ready dissociation from the lipid bilayer. It is quite possible that this domain performs a flip-flop motion into a myelin membrane packed above it, and through intercalation into the lipid bilayer it may hence play a role in fixation and tight apposition to the neighboring membrane, like the long-chain acyl group. These two structural elements could also be important in the dynamics of the spiral winding process.

This model has been substantiated experimentally in two ways. (1) The myelin membrane layers were dissociated by osmotic shock, subjected to tryptic digestion, and separated to give three large polypeptides. On sequencing these, we discovered that the endoprotease had attacked the PLP in the positions indicated by arrows in Figure 8 (top); since the enzyme cannot penetrate the lipid bilayer, this indicates that these sites are accessible on the external surface. Figure 9

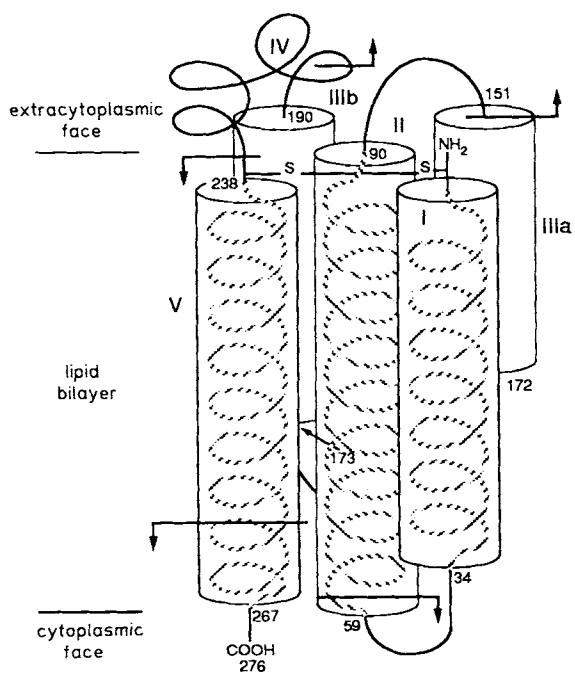
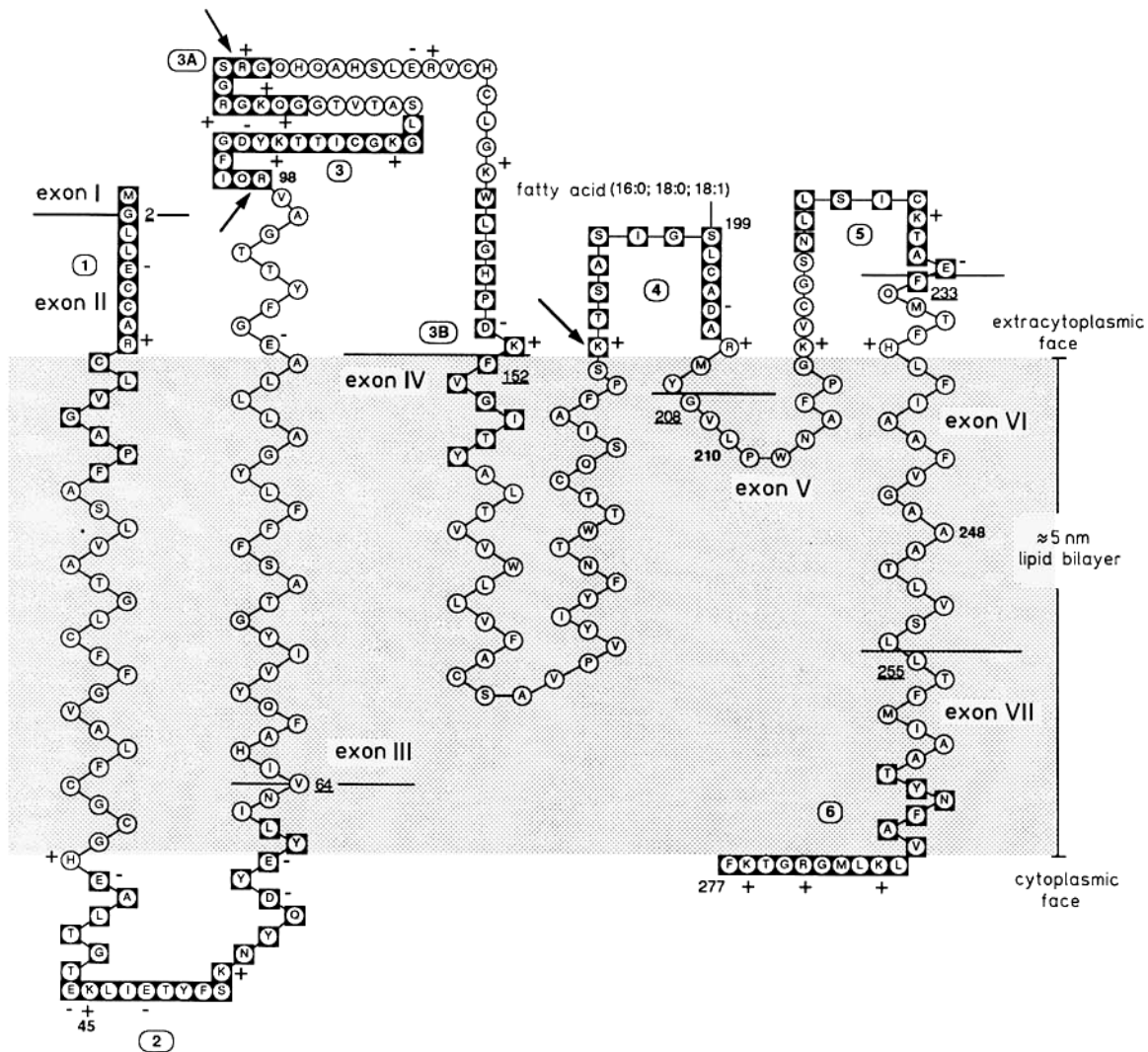


Fig. 8. Top: Model of the membrane integration of proteolipid protein, based on its hydrophobic and hydrophilic domains and on biochemical and immunotochemical evidence. The peptide sequences framed in black (1, 2, 3, 3A, 3B, 4, 5, and 6) are epitopes which were obtained by solid-phase synthesis and used to generate antibodies. Bars demarcate the exons (Section 5); arrows show points of proteolytic attack by trypsin on intact myelin whose compact layering has been loosened by hyposmotic treatment. Bottom: Suggested association of the intermembrane α -helices within the lipid bilayer, by extracytoplasmic disulfide bonds. The arrows indicate the start of each new exon.

shows the SDS-polyacrylamide gel after proteolytic treatment of the myelin. The PLP band has disappeared, giving smaller polypeptides between 7 and 10 kDa. In contrast, MBP is completely protected from proteolysis, which can only be explained by its localization in the cytoplasmic cleft, shielded by the lipid bilayers. This finding is biochemical evidence for the location of MBP in myelin.

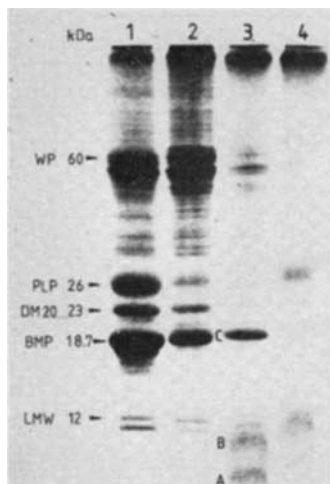


Fig. 9. SDS-polyacrylamide gel electrophoresis of myelin proteins after trypsin treatment of the intact myelin membrane. The PLP band has vanished and is replaced by proteolysis fragments. The cleavage sites are indicated by arrows in Fig. 8 above.

(2) If we accept that it is possible to generate antibodies against synthetic peptide sequences from the various domains of the PLP sequence that are marked as black boxes in Figure 8 (top) and to use them as markers of the nonpermeabilized membrane, then the orientation of PLP should be measurable histologically. For this purpose, we used primary cultures of rat brain oligodendrocytes, taken into culture, 18 days after birth. The expression of myelin proteins is similar in these cells to that in the myelinating rat. The PLP in the plasma membrane should have the final orientation

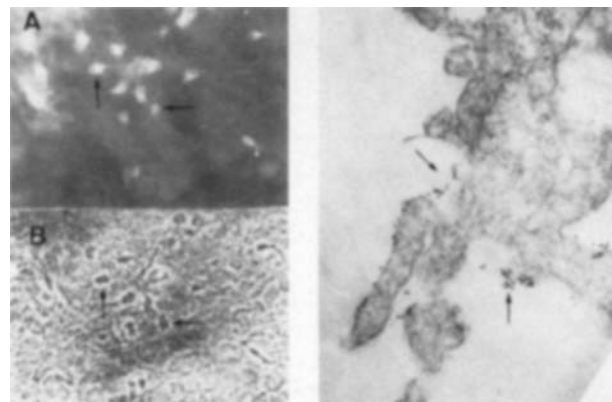


Fig. 10. Immunocytochemical localization of the PLP domains with the aid of anti-peptide antibodies. Left: A) Fluorescence labeling, B) phase contrast image. Right: Gold labeling of the oligodendrocyte plasma membrane processes in tissue culture (8150 × magnification, electron microscope).

that it will have before it segregates into the growth cone of the oligodendrocyte and on into the myelin membrane process.

Figure 10 (left) shows that only antibodies against peptides in the hydrophilic loop Arg97–Arg150 gave an immunofluorescent labeling of the oligodendrocyte plasma membranes. The same result was obtained with gold-labeled antibodies against this peptide (Fig. 10, right). Hence, both these findings agree with the proposed model for the PLP configuration in the membrane.

Surprisingly, further secondary-structure studies using the rules of *Chou and Fasman*, *Nagano*, and others revealed that all the hydrophilic domains, except for the first third of the largest domain (Arg97–Lys120), are folded as amphipathic helices. These additional secondary structures are included schematically in Figure 11. This result could be of great importance for the packing of the myelin membrane layers.

4.3. Wolfgram and Other Proteins

Further protein components, which are expressed in very low concentrations, are the Wolfgram proteins and the

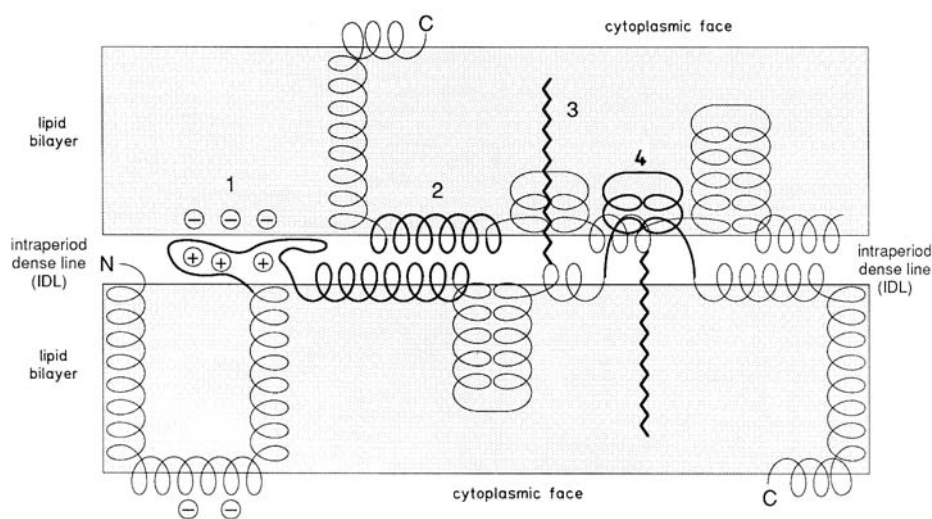


Fig. 11. Contributions to spiral winding and compact packing of the myelin layers by the interaction of (1) charged sequences, (2) the amphipathic helices of extracytoplasmic hydrophilic domains, (3) fatty acid chains, and (4) hydrophobic flip-flop loops of PLP.

“myelin-associated glycoprotein” (MAG, Fig. 6). In 1966, *Wolffgram*^[18] isolated a protein fraction from the acidic (pH 5) chloroform-methanol extract. This fraction showed three bands on SDS-PAGE, with molecular masses between 45 and 55 kDa. Of these, the 55-kDa component is α -tubulin, which reacts with specific α -tubulin antibodies in a Western blot, while the 45- and 50-kDa bands can be assigned to the enzyme 2',3'-cyclic-nucleotide 3'-phosphodiesterase.

Myelin-associated glycoprotein (MAG) is a glycoprotein with a molecular mass of 100 kDa, which is present as a trace protein (1% of total myelin protein). Its amino-acid sequence has recently been deduced from the cDNA; the sequence contains 626 amino acids (100 kDa) and in many regions is homologous to the neural cell adhesion molecule (N-CAM).^[19] Its localization in the periaxonal region of the myelin of adult rat points to possible interactions between neurons and oligodendrocytes in myelogenesis.

5. Molecular Biology of Myelin Proteins

5.1. Construction of cDNA Libraries from the RNA of Myelinating Rat Brains and the Isolation of MBP- and PLP-specific Clones

The synthesis of myelin proteins and lipids is at its greatest 18 days after birth.^[20] We isolated brain RNA from 18-day-old rats and enriched the poly(A)⁺-RNA by affinity chromatography on oligo(dT) cellulose.^[21] We then synthesized cDNA (complementary or copy DNA) with the aid of reverse transcriptase, by a modified Gubler-Hoffmann method^[22] (Fig. 12). Size fractionation by gel electrophoresis in 1% agarose afforded copies of 550- to >6000-bp double-stranded cDNA, which were cloned into the *Pst* I restriction site of the pBR 322 vector. Clones showing specificity for the proteolipid and myelin basic proteins were isolated from this bank by screening colonies by Southern-blot hybridization with labeled oligonucleotides. These nucleotides were derived from the N-terminal, C-terminal, and central regions of our PLP amino-acid sequence and from the C-terminal region of the 18.5-kDa MBP. Of these clones, the 612-bp, MBP-specific cDNA clone contained the entire coding region of the 14.5-kDa MBP isoprotein, while the longest PLP-specific clone was missing about 310 bp of the N-terminal coding sequence.^[23] The steps leading to PLP- and MBP-specific clones are summarized in the flow chart shown in Figure 12.

Using these cDNA clones, the size of the mRNA transcripts for PLP and MBP was determined by Northern-blot hybridization. Two strong, PLP-specific RNA bands corresponding to 3.2 and 1.6 kb lengths in a ratio of 2:1, as well as a weak band corresponding to 2.4 kb, were detected in 18-day-old rat brain. The mRNA's do not differ in the coding region, but contain three different 3'-nontranslated sequences; 2062 bases for the longest, 3.2-kb mRNA, 1319 bp for the 2.4-kb mRNA, and 430 bp for the 1.6-kb mRNA in the 3' direction from the stop codon. Three polyadenylation signals (AATAAA) are present, which are responsible for the varying lengths of the transcripts (Fig. 13). The second sequence required for efficient polyadenylation, TGTGTCTT,

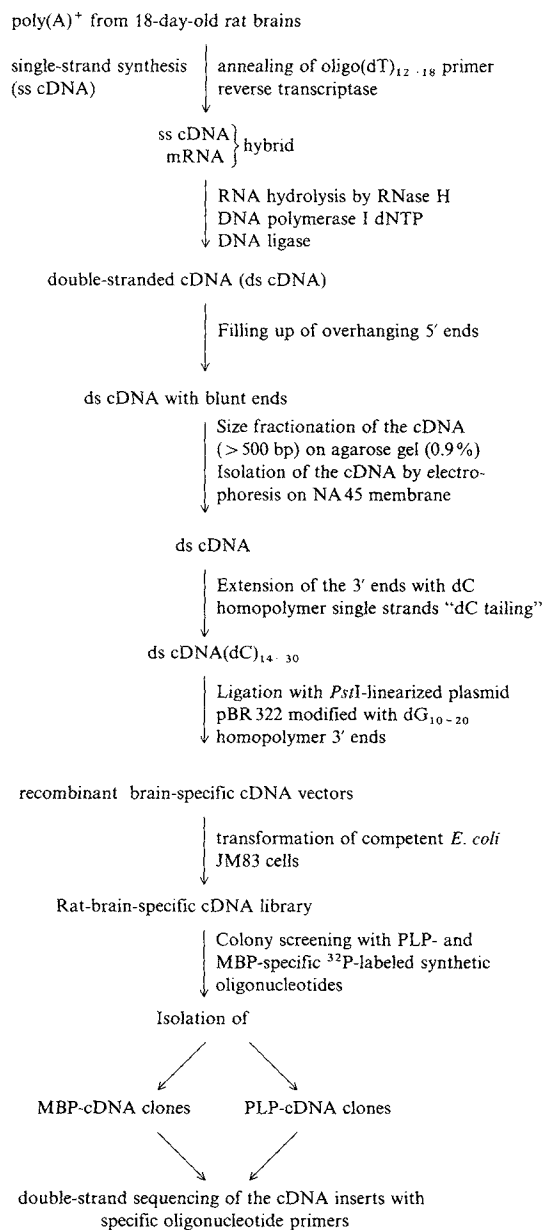


Fig. 12. Flow diagram for preparation of modified, brain-specific cDNA [22] from the brain poly(A)⁺-RNA of 18-day-old rats and for the isolation of PLP- and MBP-specific clones for DNA sequencing.

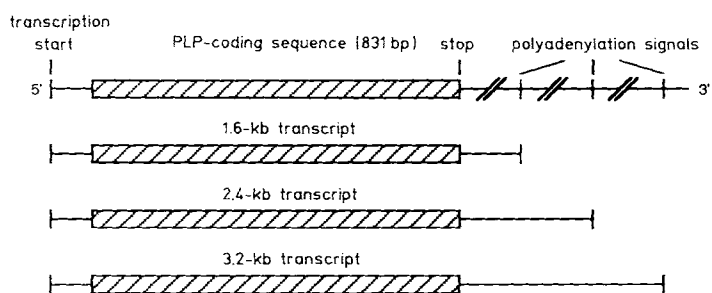


Fig. 13. Layout of the three PLP-specific transcripts. The polyadenylation signals (AATAAA) located 430 bp (1.4-kb transcript), 1310 bp (2.4 kb) and 2062 bp (3.2 kb) in the 3' direction from the stop codon are used in posttranscriptional modification.

is also present, about 30 bp downstream of the polyadenylation signal.^{124]} In humans, only the 3.2- and 1.6-kb transcripts are made.

5.2. Genetic Structure of Human Proteolipid Protein and Myelin Basic Protein

With the PLP- and MBP-cDNA clones in hand, we were able to investigate the organization of the two human genes and their chromosomal localization. To do this, we screened human genome libraries in the vectors EMBL-3 and Charon 8, using cDNA probes and oligonucleotides for the coding region and for the 5'- and 3'-noncoding ends of the exons of PLP and MBP.

Analysis of a gene, and in general of large DNA segments, is begun with the preparation of a restriction map, using type II endonucleases, which recognize specific (hexa)nucleotide sequences. With the help of hybridization probes both from the cDNA (restriction fragments) and from synthetic oligonucleotides, the position of the coding sequences (exons) and the segments between them (introns) can be deter-

mined. Further, if the 5' and 3' ends of the mRNA have been ascertained with corresponding probes, the map affords information about the size of the sought gene.

5.2.1. Exon-Intron Structure of the PLPs^{125]}

Two overlapping clones were found which contained the entire human PLP gene. Complete digestion with individual restriction enzymes and combinations of two enzymes gave characteristic fragments; logical matching up of the two genomic PLP-specific λ -phage EMBL-3 clones gave the required restriction map.

Figure 14 shows the restriction map, which was drawn up by restriction analysis and Southern-blot hybridization with [³²P]-labeled *Pst*I fragments from the PLP clone and 5'-labeled oligonucleotides. It was a great advantage at this stage that we were able to use double-stranded or supercoil sequencing^[26, 27] and, further, that the time-consuming process of sequencing could be cut short with the aid of synthetic primers from known genomic sequences. Thus, subcloning of small, overlapping restriction fragments of the DNA sequence to be screened (cDNA or genomic DNA) into the

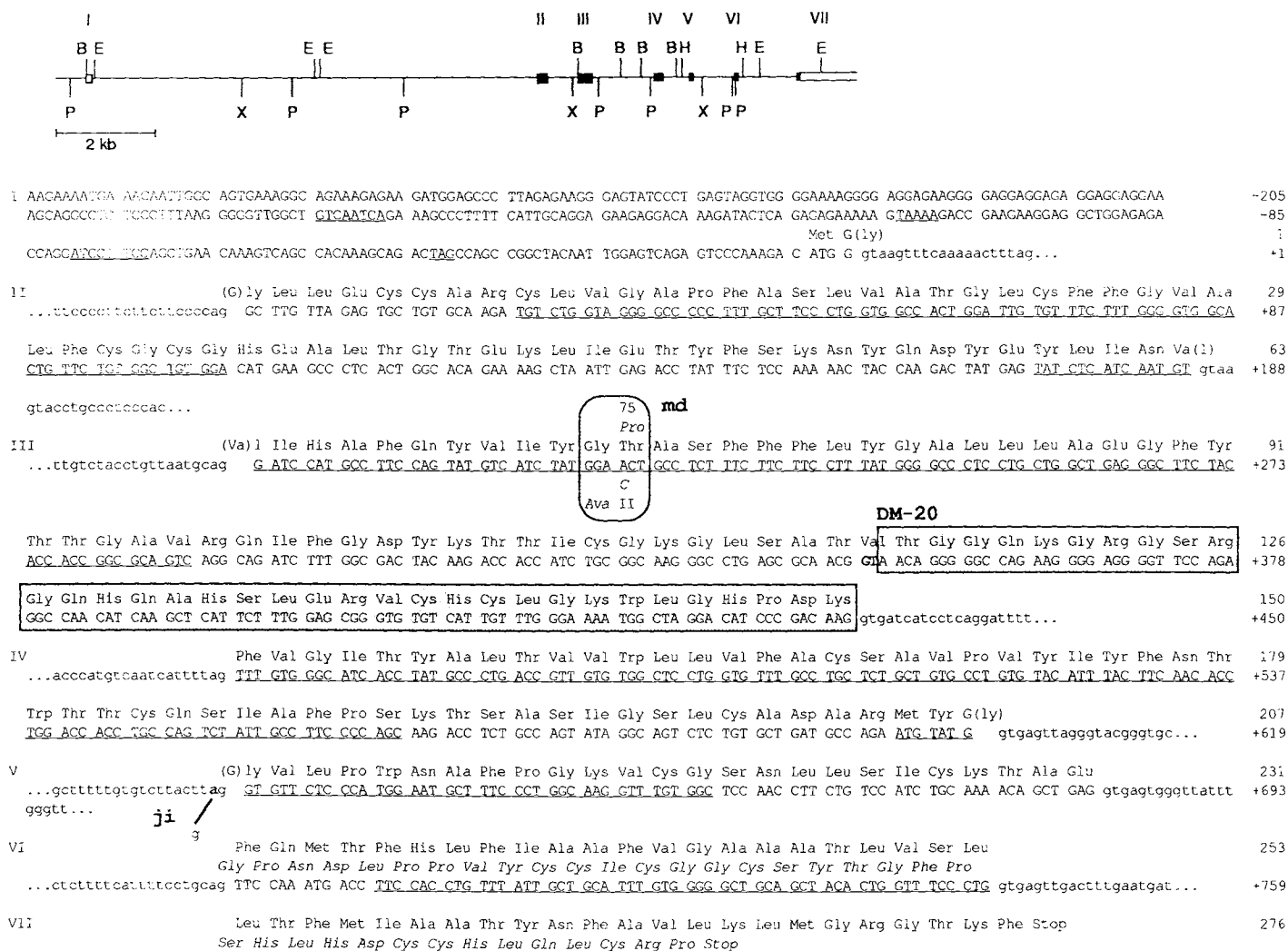


Fig. 14. Top: Restriction map and exon-intron organization of the human PLP gene. The exons are indicated by rectangles. Solid rectangles represent coding regions, open ones 5'- and 3'-nontranslated sequences. Bottom: Nucleotide sequence of the PLP exon and the adjacent intron regions. The DM-20 isoprotein and the mutation sites for jimpy mouse and md rat are shown. Restriction enzymes: B, *Bam*HI; E, *Eco*R1; H, *Hind*III; P, *Pst*I; X, *Xba*I.

M 13-phage system for dideoxynucleotide chain-termination sequencing became unnecessary. The newly obtained sequence data afforded the information needed for the oligonucleotide required as a sequencing primer.

The nucleotide sequences for the coding regions agree with the derived amino-acid sequences from the glycine in position 2 of the PLP onwards. For the glycine, however, only two of the three nucleotides were correct.

At its N-terminus, the rat cDNA sequence contains only an additional Met, compared with the mature PLP.^[28, 29] It follows that for the one amino-acid presequence of the PLP primary transcript, a further exon must exist, carrying the Met codon ATG and the first base of the glycine triplet. Downstream, GT should serve as the signal for the 5'-donor splicing sequence for the intervening intron. On the basis of the unusually high homology between the PLP sequences of human and rat, we synthesized a 24-mer oligonucleotide with 18 bases of rat cDNA and the base sequence ATGGGT, and used it as a hybridization probe. The missing exon I was identified in this way on a *Pst*I-*Eco*R1 fragment 8.8 kb upstream of exon II.

Together with the restriction map, the sequencing results yield the following picture. The human PLP gene stretches over 17 kb and consists of seven exons and six introns (Fig. 14, top). Exon I contains the 5'-untranslated region, the triplet of the Met presequence, and the first base of the glycine triplet, the N-terminus of the mature protein. From the bases following the start codon, it is clear that human PLP does not possess a signal sequence. Hence, an internal signal sequence for the primary step of integration into the membrane of the rough endoplasmic reticulum is present. The following sequences lie in the 5' region (Fig. 14, bottom): CAAT box at -174 to -170 (Met = +1), Hogness box at -115, and transcription start at -80. Exons II-VII are made up of amino acids 1-63, 64-150, 151-206, 207-231, 232-253, and 254-276. The codons for amino acids 1, 63, and 207 include the exon-intron boundaries and are hence divided between two exons, severely limiting the possibilities for alternative splicing. The entire gene is 17 kb long—since the mRNA resulting from transcription is about 3 kb, the calculated intron/exon length ratio is 4.7:1. However, since only 831 bp contain coding sequences, the ratio is 119:1. The exon-intron transition sequences described by *Breathnach* and *Chambon* (GT-AG) are also strictly conserved in the PLP gene.^[30]

5.2.2. Correlation between Exons and Protein Domains

The most interesting result arises from the position of the PLP amino-acid sequence coded in exons II-VII, not least with respect to our proposed model for integration into the lipid bilayer. Each *cis* and *trans* membrane domain and the adjoining hydrophobic regions are coded in a single exon. The C-terminal domain is an exception, being coded by two exons (VI and VII). These divisions are indicated in Figure 8 (top) by arrows.

In evolution, a variety of proteins arise by recombination of DNA sequences coding for other proteins, giving rise to special, new functions (exon shuffling).^[31] An example of this is the receptor gene for low-density lipoprotein

(LDL).^[32] To date, no polypeptide sequence with high homology to PLP has been found.

5.2.3. Alternative Splicing of PLP mRNA

Alternative splicing of primary transcripts is very pronounced in oligodendrocytes. Through the exon loss that this involves, isoforms of the myelin proteins arise. This is also true for the PLP primary transcript. The DM-20 isoform of PLP is approximately 4.5 kDa smaller than normal PLP. The detection of specific DM-20 RNA in mouse brain and the sequencing data for DM-20 mRNA indicate that 105 bp are lacking, corresponding to 35 amino acids.^[33, 34] The 212-bp-long exon III contains a cryptic splice donor sequence (GGTAAC, Fig. 14, bottom). Activation of this sequence leads to deletion of the 3' end of exon III and hence of amino acids 115-150. Nothing is yet known about how the activation of this splicing site is regulated.

5.2.4. Localization of the Human PLP Gene on the X Chromosome.

The assignment of human genes to eukaryotic chromosomes was made possible by the fusion of human and rodent cells (mouse, hamster) to give somatic cell hybrids. These contain the entire set of rodent chromosomes, plus additional human chromosomes or parts of chromosomes.^[35] The

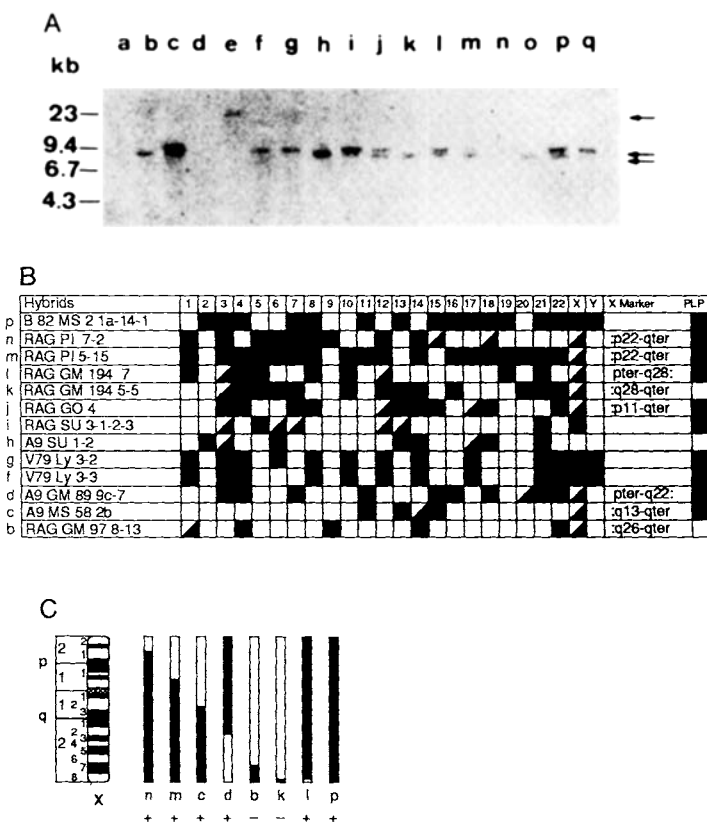


Fig. 15. Determination of the chromosomal localization of the PLP gene. A) Southern-blot hybridization of genomic human-mouse cell hybrid DNA with human-PLP-specific sequences. B) Assignment of the human chromosomes to the cell hybrids and their behavior on hybridization. C) Assignment of the PLP gene to the Xq12-Xq22 region. For details, see text.

H	Gly	Leu	Leu	Glu	Cys	Cys	Ala	Arg	Cys	Leu	Val	Gly	Ala	Pro	Phe	Ala	Ser	Leu	Val	Ala	20
R	GGC	TTG	TTA	GAG	TGC	TGT	GCA	AGA	TGT	CTG	GTA	GGG	GCC	CCC	TTT	GCT	TCC	CTG	GTG	GCC	60
		T					T														
H	Thr	Gly	Leu	Cys	Phe	Phe	Gly	Val	Ala	Leu	Phe	Cys	Gly	Cys	Gly	His	Glu	Ala	Leu	Thr	40
R	ACT	GGA	TTG	TGT	TTC	TTT	GGG	GTG	GCA	CTG	TTC	TGT	GGC	TGT	GGA	CAT	GAA	GCC	CTC	ACT	120
							A						A				T				
H	Gly	Thr	Glu	Lys	Leu	Ile	Glu	Thr	Tyr	Phe	Ser	Lys	Asn	Tyr	Gln	Asp	Tyr	Glu	Tyr	Leu	60
R	GGC	ACA	GAA	AAG	CTA	ATT	GAG	ACC	TAT	TTC	TCC	AAA	AAC	TAC	CAA	GAC	TAT	GAG	TAT	CTC	180
		T		T											G						
H	Ile	Asn	Val	Ile	His	Ala	Phe	Gln	Tyr	Val	Ile	Tyr	Gly	Thr	Ala	Ser	Phe	Phe	Phe	Leu	80
R	ATC	AAT	GTG	ATC	CAT	GCC	TTC	CAG	TAT	GTC	ATC	TAT	GGA	ACT	GCC	TCT	TTC	TTC	TTC	CTT	240
		T		T		T															
H	Tyr	Gly	Ala	Leu	Leu	Leu	Glu	Gly	Phe	Tyr	Thr	Thr	Gly	Ala	Val	Arg	Gln	Ile	Phe		100
R	TAT	GGG	GCC	CTC	CTG	CTG	GCT	GAG	GGC	TTC	TAC	ACC	ACC	GGC	GCA	GTC	AGG	CAG	ATC	TTT	300
							C								T						
H	Gly	Asp	Tyr	Lys	Thr	Thr	Ile	Cys	Gly	Lys	Gly	Leu	Ser	Ala	Thr	Val	Thr	Gly	Gly	Gln	120
R	GGC	GAC	TAC	AAG	ACC	ACC	ATC	TGC	GGC	AAG	GGC	CTG	AGC	GCA	ACG	GTA	ACA	GGG	GGC	CAG	360
H	Lys	Gly	Arg	Gly	Ser	Arg	Gly	Gln	His	Gln	Ala	His	Ser	Leu	Glu	Arg	Val	Cys	His	Cys	140
R	AAG	GGG	AGG	GGT	TCC	AGA	GGC	CAA	CAT	CAA	GCT	CAT	TCT	TTG	GAG	CGG	GTG	TGT	CAT	TGT	420
B																					
H	Leu	Gly	Lys	Trp	Leu	Gly	His	Pro	Asp	Lys	Phe	Val	Gly	Ile	Thr	Tyr	Ala	Leu	Thr	Val	160
R	TTG	GGA	AAA	TGG	CTA	GGA	CAT	CCC	GAC	AAG	TTT	GTG	GGC	ATC	ACC	TAT	GCC	CTG	ACC	GTT	480
																					T
B																					
H	Val	Trp	Leu	Leu	Val	Phe	Ala	Cys	Ser	Ala	Val	Pro	Val	Tyr	Ile	Tyr	Phe	Asn	Thr	Trp	180
R	GTG	TGG	CTC	CTG	GTG	TTT	GCC	TGC	TCT	GCT	GTG	CCT	GTG	TAC	ATT	TAC	TTC	AAC	ACC	TGG	540
		A																			T
B													A			T					
H	Thr	Thr	Cys	Gln	Ser	Ile	Ala	Phe	Pro	Ser	Lys	Thr	Ser	Ala	Ser	Ile	Gly	Ser	Leu	Cys	200
R	ACC	ACC	TGC	CAG	TCT	ATT	GCC	TTC	CCC	AGC	AAG	ACC	TCT	GCC	AGT	ATA	GGC	AGT	CTC	TGT	600
										T											C
B							T	GC							A						C
							Ala														Thr
H	Ala	Asp	Ala	Arg	Met	Tyr	Gly	Val	Leu	Pro	Trp	Asn	Ala	Phe	Pro	Gly	Lys	Val	Cys	Gly	220
R	GCT	GAT	GCC	AGA	ATG	TAT	GGT	GTT	CTC	CCA	TGG	AAT	GCT	TTC	CCT	GGC	AAG	GTT	TGT	GGC	660
B																					G
H	Ser	Asn	Leu	Leu	Ser	Ile	Cys	Lys	Thr	Ala	Glu	Phe	Gln	Met	Thr	Phe	His	Leu	Phe	Ile	240
R	TCC	AAC	CTT	CTG	TCC	ATC	TGC	AAA	ACA	GCT	GAG	TTC	CAA	ATG	ACC	TTC	CAC	CTG	TTT	ATT	720
B																					
H	Ala	Ala	Phe	Val	Gly	Ala	Ala	Ala	Thr	Leu	Val	Ser	Leu	Leu	Thr	Phe	Met	Ile	Ala	Ala	260
R	GCT	GCA	TTT	GTG	GGG	GCT	GCA	GCT	ACA	CTG	GTT	TCC	CTG	CTC	ACC	TTC	ATG	ATT	GCT	GCC	780
B			G			T															
H	Thr	Tyr	Asn	Phe	Ala	Val	Leu	Lys	Leu	Met	Gly	Arg	Gly	Thr	Lys	Phe					276
R	ACT	TAC	AAC	TTT	GCC	GTC	CTT	AAA	CTC	ATG	GGC	CGA	GGC	ACC	AAG	TTC					828
B																					

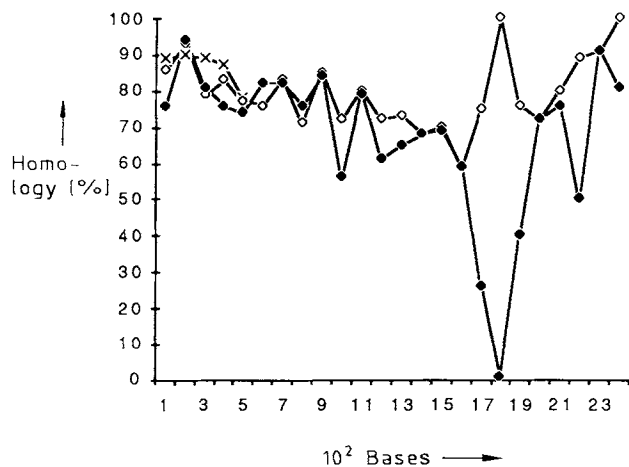


Fig. 16. Top: Comparison of human, rat, and bovine (H, R, and B) amino-acid and nucleotide-coding sequences for PLP. Bottom: Graphic illustration of homology in the 3'-untranslated region. x, bovine; o, rat; •, mouse.

human chromosomes in each hybrid cell line are defined with the aid of marker gene loci.

The genomic DNA from 15 somatic hybrid cell lines (Fig. 15A, a–q), containing all 23 chromosome pairs, was completely digested with *Bam*H1 (collaboration with Prof. Grzeschik, University of Marburg). The fragments were separated by agarose gel electrophoresis and hybridized by Southern-blot hybridization to the ³²P-labeled, 1200-bp-long C-terminal *Eco*R1 fragment of the genomic PLP clone. In Figure 15A, the human PLP-specific 9.3-kb *Bam*H1 band in the Southern blot can be distinguished (right-hand arrow, man). The smaller band (right-hand arrow, mouse) is the mouse-specific PLP band. The grid in Figure 15B shows which human chromosomes (1–22, X, Y, upper row) are present in which hybrid, either as complete chromosomes (squares) or in part (triangles). Chromosomes 2, 4, 5, 6, 7, 9, 10, 12, 13, 14, 18, 20, 21, and 22 could be excluded, since the DNA from these cell lines, in tracks b, h, and k, did not

hybridize with the PLP probe. Chromosomes 1, 3, 8, 11, 15, 17, 19, and Y were also eliminated, since hybridization occurred with DNA from cell lines which did not contain them. Hence, the X chromosome remained the sole candidate for the PLP gene locus. The assignment to the X chromosome was supported by hybridization to *Bam*H1 fragments of cell lines with four X chromosomes; strong, PLP-specific signals were clearly visible.

Narrowing down of the PLP locus to the q13–q22 region of the X chromosome was possible with the aid of somatic cell hybrids containing only part of the X chromosome. The diagram in Figure 15C shows the regions of the X chromosome contained in each cell line. Hybridizing cell lines are marked with a (+). Bars c and d reveal the smallest overlapping region between q13 and q22. The third phosphoglycerate kinase (PGK) gene is also located in this region. As confirmation, the *Bam*H1 blot was hybridized with a ³²P-labeled PGK cDNA. Parallel to our studies, the same result was obtained by Willard and Riordan^[36] and by Mattei et al.^[37]

5.2.5. Conservation of PLP during Evolution

A comparison of the amino-acid sequence and the corresponding coding nucleotide sequence for PLP from species far apart in evolution emphasizes the high level of sequence conservation. A comparison between rat, mouse, human, and, as far as possible, bovine sequences (Fig. 16, top) shows that between human and rat there are no amino-acid exchanges and only 22 nucleotide substitutions out of 831 coding bases. In mouse there are 28 base-pair exchanges, with two conservative amino-acid replacements (Ser → Thr, Tyr → Cys). This extremely high degree of conservation demonstrates the narrow range within which the protein can function. The same is also true for the 3'-noncoding sequence, where very high homology prevails around the potential polyadenylation recognition sequences (Fig. 16, bottom).

5.3. Organization of Human Myelin Basic Protein

The peripheral membrane protein myelin basic protein (MBP) occurs in several isoforms in man, mouse, and rat.^[38, 39] Thus, in rat and mouse myelin, the dominant forms are the 18.5-kDa and 14-kDa MBPs. The latter differs from the larger isoform by a deletion of forty amino acids in the C-terminal region. In the mouse, one finds a 21.5-kDa and a 17-kDa form, both with an insertion of 28 amino acids in the N-terminal region.^[10, 40]

The relative proportions of the four MBP isoforms change during mouse or rat development.^[10, 41, 42] The myelin of the human central nervous system contains three dominant isoforms, the 21.5-kDa, 18.5-kDa, and 17.2-kDa forms. The latter results from a 41-amino-acid deletion in the C-terminal region (140–180 of the 21.5-kDa form).

In Section 5.1 the isolation of a complete MBP-cDNA clone from rat brain cDNA was described. Studies in the laboratories of Hood^[11, 43] had revealed that the mouse MBP gene is distributed over seven exons, is 30 kb long, and

is located on the distal arm of chromosome 18. We isolated the human MBP gene by screening with labeled MBP-cDNA probes from genomic cosmid banks (pcos2 EMBL and Charon 4A) and analyzed its exon–intron organization. Just as for the human PLP gene, here we also carried out restriction analysis to map the MBP gene. It is distributed over seven exons and 32–34 kb.^[44] Figure 17 illustrates its structure and the sequencing strategy.

A comparison of the coding sequence of human and mouse MBP genes makes it clear that though homology in the nucleotide sequence is high, it is not as great as in PLP. Three potential transcription start sites were found by the primer extension method, at –55, –82 and –183 bp in the 5' direction from the translation start. In the 5'-noncoding region there is neither a TATA box, which is often found in eukaryotic genes, nor a CAAT box. However, there are three direct "repeats", a nonameric sequence and two octameric nucleotide sequences. A decameric sequence at –256 to –265 is absolutely homologous to one in the regulatory region of the PLP gene. Further studies will show whether these motifs are important in transcriptional regulation. The isoforms of MBP arise by alternative splicing. The exons involved here are basically exons II, V, and VI. Figure 18 summarizes the splicing process and the isoforms that result.

6. Animal Models in the Study of Normal and Genetically Defective Myelin Membranes of the CNS (Dysmyelinoses)

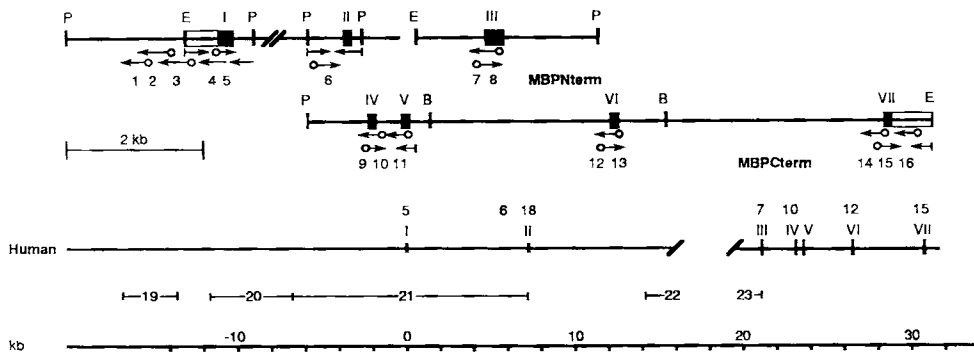
Animal models possessing a genetically determined defect in myelin membrane synthesis are extremely useful in (1) investigation of membrane structure and the function of membrane components, especially proteins, (2) analysis of the differentiation process in myelogenesis, and (3) studies of pathogenesis on a molecular level. Myelin mutants of mouse, rat, rabbit, and spaniel are known; two sex-chromosome-linked mutations of mouse and rat will be described.

6.1. Sexually Inherited (X-Chromosomal) Defects

6.1.1. *Jimpy (ji) Mouse*

In 1952, Falconer described the Tabby (Ta) marker in mouse.^[45] Heterozygous females are distinguished by horizontal stripes on the back, while homozygous males have a light brown coat. The jimpy gene is linked to the Ta marker; it leads to a complete absence of myelin in the affected male mouse and to an early death with symptoms of tremors in the entire striated muscle and of cramps. Females carrying the ji gene display a mosaic pattern, since expression of the X-chromosomal gene is dependent on inactivation of either the mutant or the normal X chromosome.^[46, 47] While hypomyelination is compensated for with increasing age in heterozygous females, protein chemical analysis of the brain of affected males shows a marked reduction in PLP and MBP.^[48, 49]

The primary effect of the ji mutation was sought first in PLP expression. Southern blots of genomic DNA from ji and



I

... tgggtagggtgggtgtgtgatggatggatagatggatggatgggttaaatggactgttatgtggatggatggatggatggatagagagatagatggatgactgtattacagg
gatatgtgagtgaaatcctgtttctgtagataaagtaagatgattggagaggaactaactaaatgatatttattaaacctaacactctaacctgaaagcaaatggatcattgcc
ttcgtgacagaaatgtggtattttttggagaagctatgagatgctggtatatacaatgaaatctctcaatcccactccagatttctaatgtttctgctccagagaggaagccaagt
caaaatgtcctgaataagcagtctctattgtgagagccctctgtggaatctgggattgaacaatctcaaatgcccactcttctcatgcatgaattgcaaaaagatgtggcaagt
ttgtttctccaagaactaaacacaccttttgcaaaataatgctccttgcatatttaacttatgaccagtgcccttttaaacagtgcaatgtccatcaagggtgctgacacatctg
ggctctccgggagcagcctggcagcaccgggaacagctgatgtgctgctgcatgctcagatgactctcatcggaagcctgggtgcattttacgctgggtgccaactctgag
taactgaggaatcccagacctctgaaacacagagctgcaataggctgctccatccaggttagctccatctaggccaaggctttatgaggactgcaatattctgtgggttta
taggagacagctaggccaagccctcagagaaagctgctttgctcgggtgctcagctttgcaagccctgattcatatctcattgtgtttgaggagggcagatgcaacccaagac
aatgggacctctcagagacacagcgggtgactgactccaagcgcacagcggcaagaaatgctggcagagatgccaccagctgaccagggagcggcccacttgatccgctc
tttcccgagatgcccggggaggaggaacaacctccaagacagccctctgagtcgagcagctccagaccctccaagaagcagtgccaccactccgagagcctggatgtg

Met Ala Ser Gln Lys Arg Pro Ser Gln Arg His Gly Ser Lys Tyr Leu Ala Thr Ala Ser Thr Met Asp His Ala Arg His Gly Phe Leu 29
ATG GCG TCA CAG AAG AGA CCC TCC CAG AGG CAC GGA TCC AAG TAC CTG GCC ACA GCA AGT ACC ATG GAC CAT GCC AGG CAT GGC TTC CTC 87

Pro Arg His Arg Asp Thr Gly Ile Leu Asp Ser Ile Gly Arg Phe Phe Gly Gly Asp Arg Gly Ala Pro Lys Arg Gly Ser Gly Lys 58
CCA AGG CAC AGA GAC ACG GGC ATC CTT GAC TCC ATC GGC CGC TTT TTT GCG GGT GAC AGG GGT GCG CCC AAG CGG GCT GCT GGC AAG gtga 174

gctctgaggagtagaggatttttagtttaaatggaagcaagagaaatcagtaggtgaaactcagccattagaggaagaactggcagctagcctctgtctgctaaaggtctcgtctcc
gtgctggagaatgcatatgagcccaagagtgtggcctgagaggtgcttaggacgtttctggttaactcaccctctcttctccacaagggatggtggcgggtgtgctcaggaat
gtaaggacatgctgaattc...

II

... ctgcagaatcggaaaaggtcctcctcgttccactgaaacctcacagagcagaaaagctttaaactgctaaatccaatgcagaagataaacacactgctataaaagaaaaat
acaactctgcaagtgaatggaatgaaatctatccatccatcctgtagagctcaaaaaaccttttagtgcactttgctccagactgggaagggcctctcgcactggatcctagaat
ctttacagctggtgctcctgctccatataaagaactcttggctccatgtttgatcacagggcctcagaatgactttggaggagagaatctctccctaaactttctctctcgtctcgt
tctcaggtcctcagggcagctgctcctctgactccatcactcttggctcttctccatccatctgcaatgctctctctcctcctgctcctcctccacc
ccccctcactcctcctcactctgggctcttgcaagccagctctagaggagatttggtaggagctttggggcattgcccggcgcccaccggactcacgagccactcctgtgctc

Val Pro Trp Leu Lys Pro Gly Arg Ser Pro Leu Pro Ser His Ala Arg Ser Gln Pro Gly Leu Cys Asn Met Tyr Lys 84
ccccggcag GTA CCC TGG CTA AAG CCG GGC CGG AGC CCT CTG CCC TCT CAT GCC CCG AGC CAG CCT GGG CTG TGC AAC ATG TAC AAG gtaag 252

acgcggggggtctcaccatcggggcaggggtgactgctcctgagctctcagccgactgctcctcggggcaggtgctcactgccaggggcccaccaccagcct...

III

... ttcctcagggagcaagccgaggactgtggaactgtcctgaggtcaccgcccctctgttttcag Asp Ser His His Pro Ala Arg Thr Ala His Tyr Gly 96
GAC TCA CAC CAC CCG GCA AGA ACT GCT CAC TAC GGC 288

Ser Leu Pro Gln Lys Ser His Gly Arg Thr Gln Asp Glu Asn Pro Val Val His Phe Phe Lys Asn Ile 119
TCC CTG CCC CAG AAG TCA CAC GGC CGG ACC CAA GAT GAA AAC CCC GTA GTC CAC TTC TTC AAG AAC ATT gtaagtacgatcgtatgggaagaggtga 357

gcaactgtgagggggaggagggg...

IV und V

Val Thr Pro Arg Thr Pro Pro Pro Ser Gln Gly Lys 131
... gccaggggtctctgtgctcttcag GTG ACG CCT CGC ACA CCA CCC CCG TCG CAG GGA AAG gtaagacctggaatggtttgattgatcacttttctgata 393

gaccttctcaaaatcccataatgtaccaagagagagttaggctccagactaccagaatccatcccacagctggtgccagcagctcccaagtagaacaggtcggagatccatgac
cctcctgtcctccgcacatgcacagccgctgtggccctagctcggccccctcggagctccgggtggaacctgttttaccacctcagctcactgtgctttgactgtgttccct

Gly Arg Gly Leu Ser Leu Ser Arg Phe Ser Thr 142
GAG AGA GGA CTG TCC CTG AGC AGA TTT AGC TGG gtagggtgac 426

gaacgacttccatcggtctcctcctccagctccacagccccgaaactttgtgtctgctctgttctcgttctcctggctcctgctcctctctctctctctcga...

VI

... cctcagcgtggtgctggccggtgctcctgaacctcaccagctcagctcgggctggccctcccggggcccctggtggcagctccagtggtcacaagcagcgtgccagcagc

Gly Ala Glu Gly Gln Arg Pro Gly Phe Gly Tyr Gly Gly Arg Ala Ser Asp Tyr Lys Ser 162
cgcggttgagaggttgagctcctggttctctcttcag GGG GCC GAA GGC CAG AGA CCA GGA TTT GGC TAC GGA GGC AGA GCG TCC GAC TAT AAA TCG 486

Ala His Lys Gly Phe Lys Gly Val Asp Ala Gln Gly Thr Leu Ser Lys Ile Phe Lys Leu 182
GCT CAC AAG GGA TTC AAG GGA GTC GAT GCC CAG GGC ACG CTT TCC AAA ATT TTT AAG CTG gtaaggtaccctctgctcagctccactga... 546

VII

... agaaaatgctcatcaagcaagcaatggagcgggtgcaactcaccacagaatgcaactgtttgagagcagctggtatgccagggcaccctcctgggctgggaatccgattc
cagttctctcaccagaaactgaaatcattagcatttctgctgaggaggtcgggagaatggaatgaaagaccagctctccggggtgccatttctattagcagatgagagagacccc

Gly Gly Arg Asp Ser 187
aatggctcagcatggaccgggaccacagaaggggagctggtgtggggagaccctggcgaactctgctcctaacctcctctctctctctctcttcag GGA GGA AGA GAT AGT 561

Arg Ser Gly Ser Pro Met Ala Arg Arg Stop 196
CGC TCT GGA TCA CCC ATG GCT AGA CGC TGA aaaccacctggtccggaatcctgctcctcagcttcttaataataactgcttaaaactttaaactcccactgcccctgtt 588

acctaattagagcagatgaccctccctaatgctcggaggtgtgcaactgtagggctcagggcagccagcctaccggcaattccggccaacagttaaatgagaacatgaaaca 607
gaaaacggttaaaactgctctctgtggaagactcctctcccgcgaatgtgcccacagcagcagctgggtcttcagggggcccaggtgcaacagcgtccctccacgttcacc 726
ctccacccttgactttctttctcggcgtgctcggcacccttgctctttgctggtcactccatggaggccacacagctgcagagacagagagcagctggggcagagagagcagctgtt 845
gacatccaagctcctttgttttttttctctctctcct 964
ggtatgtgacatgagggtggcagctgttagagtcacagctggggcagcagagagggggccacctcccagggcctggctgcccacaccccacttagctgaattc... 1074

Fig. 17. Top: Exon-intron organization of human MBP gene. Bottom: Nucleotide sequence of the exons and extensive sections of the introns of the MBP gene. Enzymes as in Fig. 14.

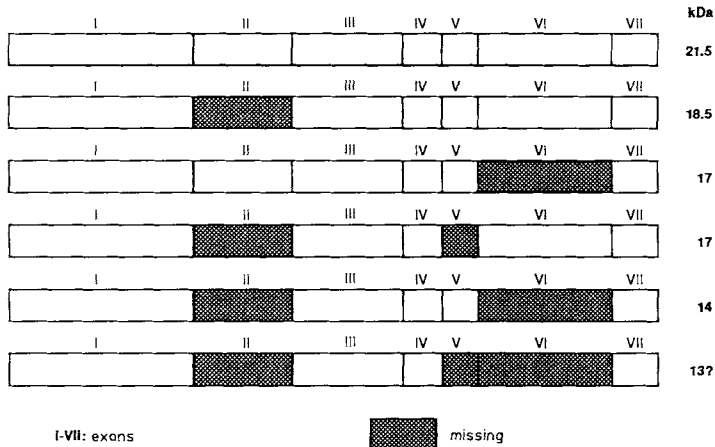


Fig. 18. Isoforms of myelin basic protein arise by alternative splicing. The molecular masses are given in kDa on the right; the exons eliminated by splicing are hatched.

normal mice with PLP cDNA proved to be identical.^[34, 37, 50, 51] Exact determination of the *ji* defect in the mRNA was furnished by isolation and analysis of *ji*-PLP cDNA.^[50] A 74-base-pair deletion was discovered, with a shift in reading frame at the C-terminus of PLP.

A glance at the exon-intron structure of the human PLP gene shows that the 74-base deletion corresponds exactly to the nucleotide sequence of exon V. The most obvious interpretation was an alternative splicing (Fig. 14, bottom). Indeed, there is a transition at the splice acceptor site (AG → GG), which eliminates exon V, intron IV, and intron V. Exon V ends on the first nucleotide of the glycine (G). Since exon VI starts with the triplet TTC (Phe), a frameshift occurs, leading to synthesis of a missense protein. The result

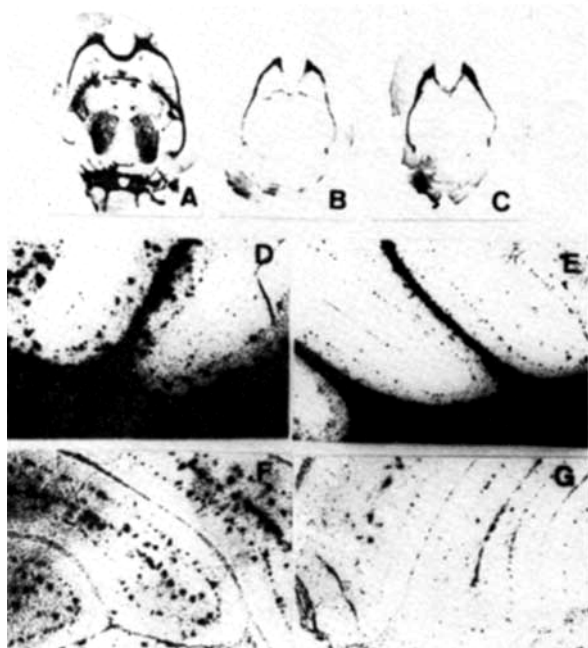


Fig. 19. In situ hybridization of horizontal cryosections of normal and *md* rat, and of *jimpy* mouse, with antisense PLP and MBP RNA. A, rat; B, *md* rat; C, *jimpy* mouse; D, normal rat hybridized with antisense PLP RNA; E, hybridized with anti-MBP RNA; F, *md* rat hybridized with antisense PLP RNA; G, hybridized with anti-MBP RNA.

is the loss of myelinated oligodendrocytes and the appearance of immature oligodendrocytes. This is easily recognizable on comparative in situ hybridization of normal, *md*-rat, and *ji* brain sections, using antisense PLP and MBP mRNA (Fig. 19).

The disease takes a less dramatic course in the myelin synthesis deficient (*msd*) mouse, which is phenotypically very closely related to the *ji* mouse.^[52, 53] This mutation is an X-chromosome-linked defect as well. It consists of a single base transition (C → T) in exon IV leading to a homologous amino-acid substitution (alanine → valine) in PLP.^[69]

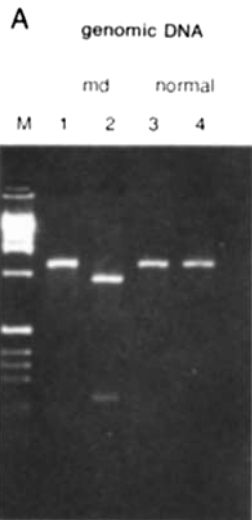
6.1.2. Myelin-Deficient (*md*) Rat

The *md* rat is a mutant of the Wistar rat, which in phenotype is very closely related to the *ji* mouse. The endoplasmic reticulum of the CNS oligodendrocytes is expanded, and fluffy precipitates appear in the cytoplasm.^[54] The mRNA of PLP and MBP, and of MAG and CNP, is greatly reduced. Figure 19 compares the in situ hybridizations we performed on brain sections of normal rat, *md* rat, and *jimpy* mouse, using [³⁵S]UDPS-labeled antisense PLP and MBP RNA.^[55] The markedly reduced number of oligodendrocytes in *md* and *ji* brain is recognizable from the insignificant labeling by the specific hybridization probes.

In order to investigate the genetic defect on a molecular level, Southern blots of normal PLP DNA and of *md* rat were compared. No size differences were observed; the sequences of the 5'-regulatory region and those of exons IV to VII and introns IV to VI were identical. We isolated nucleotide sequences coding for exons I, II, and III from the *md*-rat-brain-specific cDNA library by the polymerase chain reaction (PCR) method and, at the same time, amplified exon II, intron II, and exon III with suitable oligonucleotide primers. Sequencing of the PCR fragments of the *md* cDNA revealed a point mutation (A → C transversion), leading to the mutation of Thr 75 into Pro. The point mutation lies in exon III, the sequence coding for the second transmembrane α -helical segment. This transversion generates an *Ava*II restriction site (GGACC), and the resultant *Ava* polymorphism in exon III constitutes a rapid diagnostic test for the *md* allele (Fig. 20). What are the consequences of this point mutation for the protein structure? Proline, with its preceding glycine, breaks the α -helix structure and leads to a bend and a partial β -turn structure in the helix. This conformation clearly hinders the integration of the C-terminal PLP sequence into the lipid bilayer of the myelin. On a cell biological level, this A → C transversion (i.e., the mutation of one out of 17 000 bases) finds expression in the loss of oligodendrocytes. Myelination does not take place, and this leads to the early death of the affected male animal. We are investigating this pathogenetically important chain of reactions very intensively at the moment.

6.2. Autosomally-Recessively Inherited Dysmyelinoses

One recessively inherited dysmyelinosis is the *shiverer* defect in mouse (*shi*). This defect arises from the deletion of five of the seven exons of the MBP gene, which is located on chromosome 18, q22-qter.^[43, 56, 57] The loss of MBP still



B

64	IleHisAlaPheGlnTyrValIleTyrGlyProAlaSerPhePheLeuTyrGlyAla	83
314	GATTCATGCTTTGCCAGTATGTCATCTATGGACCTGGCTCTTTCTTCTTCCTTTATGGGGCC	373
	Ava II	
84	LeuLeuLeuAlaGluGlyPheTyrThrThrGlyAlaValArgGlnIlePheGlyAspTyr	103
375	CTCCTGCTGGCCGAGGGCTTCTACACCACCGCGCTGCAGGCATGATCCTGGCGACTAC	434
	Sau 3A	
104	LysThrThrIleCysGlyLysGlyLeuSerAlaThrValThrGlyGlyGlnLysGlyArg	123
435	AAGACCACCATCTGGCGCAAGGGCCCTGAGCGCAACGGTAACAGGGGGCCAGAAGGGGAGG	494
124	GlySerArgGlyGlnHisGlnAlaHisSerLeuGluArgValCysHisCysLeuGlyLys	143
495	GGTTCCAGAGGCCAACATCAAGCTCATTCTTTGGAGCGGGTGTGCATGTGTTGGGAAAA	554
144	TrpLeuGlyHisProAspLys	150
555	TGGCTAGGACATCCCGACAAG	575

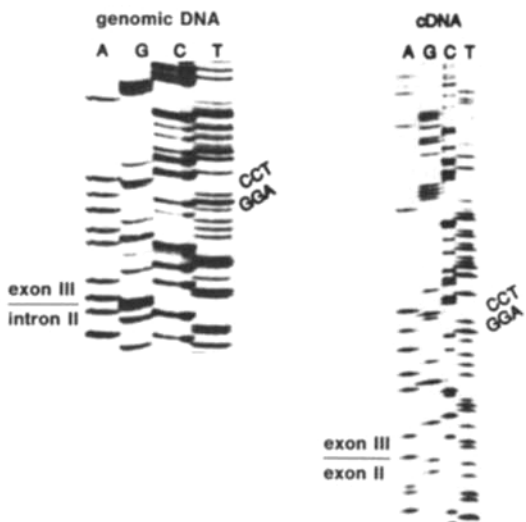


Fig. 20. A) Amplification of exon II-intron II-exon III by the polymerase chain reaction (PCR), using genomic DNA of wild-type and md rat as template (md 1 and normal 3). Restriction of the resulting 1180-bp fragment with *Ava* II. An *Ava* II restriction fragment length polymorphism is apparent. *Ava* II cleaves the fragment derived from the genomic DNA of the md rat into a 960-bp and a 220-bp fragment (md 2), but does not attack the fragment from the genomic DNA of the normal rat (normal 4). B) Nucleotide sequence and derived amino-acid sequence of exon III of the md-rat PLP gene (see also Fig. 16). Sequencing gels of genomic and cDNA from md rat.

permits myelin formation, but the compact cytosolic gap visible under the electron microscope as the main dense line (MDL, Fig. 3) does not develop.^[58] This myelination defect

was overcome by implanting the intact MBP gene into the germ cells of the mouse in a transgenic model.^[59]

A further autosomal mouse mutant is the myelin-deficient mouse. Hood's group has found that, due to an MBP gene duplication and inversion, regulation of gene expression is disturbed, yielding a phenotype similar to that of the shiverer mutant. Here, too, it was possible to generate transgenic mice which made myelin to different extents, by introducing the normal MBP gene into the cells.^[60]

The quaking mouse (qk) is the result of a defect linked to chromosome 17. Phenotypically, one sees a much relaxed myelin structure under the electron microscope, with greatly reduced expression of both the PLP and MBP genes. MBP does not seem to be built into the myelin membrane. A molecular biological explanation of this mutation is still awaited.^[49, 61]

6.3. Sex-linked Recessive Human Dysmyelinoses

Demyelination leads to the degradation of the existing, intact myelin by inflammatory or toxic agents. In contrast, a series of dysmyelinoses, the leucodystrophies, are the result of genetically conditioned functional disorders in the oligodendrocytes. Human dysmyelinoses with X-chromosomal recessive inheritance (e.g., adrenoleucodystrophy (ALD) and "familial diffuse sclerosis", also known as Pelizaeus-Merzbacher disease) are of special importance in this context.^[62] In homozygous, male descendants, the severe form, adrenoleucodystrophy, leads to early mental retardation, motor disorders, demyelination of the optic nerve, and blindness, and to death at an age of four to eight years. Characteristic here is the accumulation of very long chain fatty acids ($>C_{24}-C_{26}$) in almost all the tissues, usually as their cholesterol esters.^[63] This is used as a diagnostic aid. Gas-chromatographic determination of the long-chain fatty acids in the lipids of leucocytes, skin fibroblasts and cells obtained by amniocentesis is at present the diagnostic method of choice, especially prenatally.^[64] The ALD locus on the X chromosome is not yet exactly determined, but a DNA probe specific for the Xq28 band contains a restriction fragment length polymorphism (RFLP) which is said to be characteristic for the defective allele.^[65] However, as long as the exact distance between this probe and the ALD locus is unknown, an uncertainty factor is attached to this RFLP because of possible recombination.

Pelizaeus-Merzbacher disease is a rare form of leucodystrophy. Mental and physical decay begins in infancy and leads to death in the first years of life. The phenotype is very similar to that of *ji* mouse or md rat. The disease is histologically characterized by a complete lack of white matter in the CNS. Astrocytes in the dysmyelination region reveal fat globules. The defect postulated in phospholipid metabolism^[66] is certainly only a peripheral symptom in the complex phenotype of this genetically determined dysmyelinosis. The X-chromosomal linkage, coupled with the complete absence of proteolipid protein^[67] and the great immunocytochemical changes in marker enzymes for myelin, points to a mutation in the PLP gene. Cloning and analysis of the Pelizaeus-Merzbacher PLP gene has led to an understanding of the mutation and the pathogenesis of the disease

in four different families: a C → T transition in exon IV leading to a threonine 155 exchange by isoleucine^[7a] and proline 14 → leucine,^[71] tryptophan 162 → arginine,^[72] and proline 216 → serine^[73] substitutions.

6.4. Demyelinating Diseases

The commonest and most serious inflammatory disease of the CNS, which very often takes a gradual course, is encephalomyelitis disseminata, also known as multiple sclerosis (MS). Its etiology is still quite unclear, although viral infections—more than twenty have by now been described—are regularly cited as the triggering event. This is especially true of the chicken pox, German measles, and mumps viruses, and, most recently, the human retrovirus HIV-1.^[68] An autoimmune reaction plays a significant part in pathogenesis. In animal models it is possible to generate a symptomatically related demyelination experimentally by immunizing rabbits or rats with myelin basic protein. In addition to the sites of inflammatory degeneration that appear in this experimental allergic encephalitis (EAE), T lymphocytes with MBP specificity are activated in the test animal. Transfer of the T lymphocytes to a healthy animal can trigger symptoms of multiple sclerosis. The cerebrospinal fluid of MS patients also contains MBP-specific T lymphocytes, analogously to the animal model.

Independently of the etiology, one can ask whether MBP is the primary antigen for triggering the autoimmune process. In trying to understand pathogenetic events, it is a great help to know the molecular architecture of structures involved in the process. MBP is quite clearly located within the cytoplasmic space of the myelin membrane, where it is shielded from protease attack by the dense lipid bilayers, as has been shown experimentally.^[14] If one looks at the myelin membrane model (Fig. 8A), it becomes clear that the proteolipid protein (PLP) has large, hydrophilic domains exposed at the membrane surface, where they are directly accessible as a primary point of attack for the proteases of macrophages, lymphocytes, and leucocytes. Fragmentation of PLP would severely disrupt the membrane organization of the myelin, and this could expose phospholipids to phospholipase attack and, as a result, the myelin basic protein to proteases. The high antigenicity of MBP and its peptide fragments play a dominant role in the autoimmunization process, but only a secondary one in this hypothetical sequence of events, and at a later stage in the pathogenetic process. A knowledge of the crucial epitopes that are recognized primarily by activated T lymphocytes in the demyelination process could be of great importance in understanding the pathogenesis of multiple sclerosis and in its therapy, even if the etiology is not yet fully explained.

7. Summary and Perspectives for Membrane Research in Neurobiology

Because of its relatively small number of components, the CNS myelin membrane is one biological membrane whose morphology and function on a molecular level have largely

been described. Chemical and biochemical analysis has revealed that the simple and complex myelin lipids that make up the 5-nm-thick bilayer are the decisive factor in the insulating characteristics of the myelin sheath around the axons. The dense lateral packing of the sphingolipid long-chain fatty acids and the cholesterol in the lipid bilayer is stabilized by a network of hydrogen bonds, described here for the first time. This network is built up between the polar groups at the interphase between the hydrophobic core of the bilayer and the polar heads of the lipids.

The conspicuously high content of acidic polar head groups—one anionic to four polar or zwitterionic—leads to a polyanionic cytoplasmic and extracytoplasmic surface. Both will be involved in ionic interactions. Biochemical and immunotopochemical studies have further revealed that the myelin basic protein in the cytoplasmic space is not accessible from the exterior. Through ionic interactions of the side chains of its basic amino acids with the anionic polar head groups of sulfatides and phospholipids, but also with an anionic domain of proteolipid protein, the MBP causes a compact layering of the oligodendrocyte plasma membrane processes. This is seen in the electron-dense main dense line (MDL) under the electron microscope. Ionic interactions between polar head groups of the lipid bilayer and domains of proteolipid protein must be responsible for the dense packing on the extracytoplasmic side, between the external surfaces of the tightly wrapped myelin processes. This narrow cleft appears in the electron microscope as the intraperiod dense line (IDL). In addition, hydrophobic interactions may occur between opposing membrane surfaces, due to long-chain fatty acid residues. For example, they form an ester bond to Thr/Ser 198 of PLP and can intercalate into the hydrophobic phase. The hydrophobic sides of amphipathic helices could also affect the pattern of outer membrane adhesion surfaces, as could the flip-flop dynamics of a small hydrophobic *cis* loop in the poorly understood spiral winding process (Fig. 2B). Either of these could be a significant stabilizing factor in formation of the dense, multilamellar membrane system. This system is not only responsible for myelin's insulating function, but also for saltatory excitation along the nodes of Ranvier, which proceeds by depolarization of only small areas of the axonal membrane.

The myelination of the CNS axons is a fascinating process of development and differentiation within brain maturation. Following a program that is regulated both in time and in space within the individual regions of the brain, the mass of lipids and myelin proteins is synthesized within a short time span (2–3 weeks in rodents, 1–2 years in humans).

Using the molecular-biological techniques described here, we can now analyze the course and regulation of myelinogenesis and resolve both the controlling elements and factors and the expression of genes coding for myelin membrane proteins and enzymes responsible for synthesis of the complex myelin lipids. *In situ* hybridization techniques will play a large role here, as will analysis of DNA–protein interactions in the regulatory regions of the genes described. Thus, we will be able to tell whether the gene activity for myelin proteins is “switched on” simultaneously and in conjugation with lipid synthesis, how the myelin building blocks are transported to the axon, where the segregated membrane components of the oligodendrocyte plasma membrane

myelin process are combined. In vitro protein synthesis of PLP and MBP and integration of PLP into the lipid bilayer are currently under experimental investigation, in order to gain understanding of the in vivo process.

Analysis of the genetically determined myelin defects (dysmyelinoses) described here, the jimpy mouse and md rat, furnish convincing evidence of the far-reaching possibilities for molecular biological techniques. They can be used for elucidation not only of defects at the DNA level and their chromosomal locations, but also of the cell biological basis for the pathogenetic process arising from the mutation. Thus, we will soon know why erroneous expression of a structural protein such as PLP causes death of the oligodendrocyte, failure to myelinate, and the early death of the individual. The animal models studied are of eminent importance in explaining analogous dysmyelinoses based on defective myelin synthesis in humans.

A large number of genetically determined myelin defects in animals and in man await the elucidation of the relevant mutations. Transgenic animal models will be indispensable in understanding the pathogenic process in these brain diseases. Elucidation of the myelin membrane topochemistry and the availability of the protein structures has given an important thrust to research on demyelinating diseases, with multiple sclerosis (encephalomyelitis disseminata) the primary example. This is true above all for the autoimmunological aspects of this disease. The antigenic epitopes of the myelin target structures can now be determined, opening up extensive therapeutic possibilities.

The results that have been achieved in biochemical and molecular biological research in recent years in the field of neurobiology, as documented here for the CNS myelin membrane, provide impressive evidence that a solid chemical and biochemical knowledge of macromolecular structure is first required. With the aid of molecular and cell biological techniques and reasoning, it is possible to learn to understand the normal functions linked to these structures and their pathological alterations. The "new biology", in the widest sense, makes molecular neurobiology one of the most exciting fields in biology today.

Our research described in this review article was generously supported by the Deutsche Forschungsgemeinschaft (SFB 74), the Bundesministerium für Wissenschaft und Forschung (Gene Centre, Cologne), and the Fritz-Thyssen-Stiftung. My special thanks go to all the co-workers mentioned and to Dr. B. Tunggal and Dipl.-Chem. K. Hofmann for fruitful and enthusiastic collaboration in a field of neurochemistry that requires a high level of experimental skill. I am grateful to Jochen Teufel for help in preparing the diagrams and the manuscript.

Received: November 17, 1989;
revised: February 13, 1990 [A 779 IE]
German version: *Angew. Chem.* 102 (1990) 987
Translated by Michael Kertesz, Zürich

[1] R. Virchow, *Virchows Arch. Pathol. Anat. Physiol.* 6 (1854) 562–572.
[2] M. L. Ranvier: *Leçons sur l'Histologie du Système Nerveux*. Librairie F. Savy, Paris 1878.
[3] A. L. Hodgkin, A. F. Huxley, *J. Physiol.* 117 (1952) 500–544.
[4] T. V. Waehneltdt, J. M. Matthieu, G. Jesrich, *Neurochem. Int.* 9 (1986) 463–474.

[5] P. I. Yakolev, A.-R. Lecours in A. Minkowski (Ed.): *Regional Development of the Brain in Early Life*, Blackwell, Oxford 1967, pp. 3–70.
[6] W. T. Norton, W. Crammer in P. Morell (Eds.): *Myelin*, Plenum Press, New York 1984, pp. 147–195.
[7] Y. Oshiro, E. H. Eylar, *Arch. Biochem. Biophys.* 138 (1970) 392–396.
[8] E. Eylar, pp. W. Brostoff, G. Hashim, J. Coccam, P. Burnett, *J. Biol. Chem.* 246 (1971) 5770–5784.
[9] P. R. Carnegie, *Biochem. J.* 123 (1971) 57–67.
[10] E. Barbarese, P. E. Braun, F. H. Carson, *Proc. Natl. Acad. Sci. USA* 74 (1977) 3360–3364.
[11] N. Takahashi, A. Roach, D. B. Taplow, S. B. Prusiner, L. Hood, *Cell* 42 (1985) 139–148.
[12] J. Kamholz, F. de Ferra, C. Puckett, R. A. Lazzarini, *Proc. Natl. Acad. Sci. USA* 83 (1986) 4962–4966.
[13] P. E. Braun in P. Morell (Ed.): *Myelin*, Plenum Press, New York 1984, pp. 97–106.
[14] W. Stoffel, H. Hillen, H. Giersiefen, *Proc. Natl. Acad. Sci. USA* 81 (1984) 5012–5016.
[15] W. Stoffel, unpublished results.
[16] G. L. Stoner, *J. Neurochem.* 43 (1984) 433–447.
[17] J. Folch, M. Lees, *J. Biol. Chem.* 191 (1951) 807–817.
[18] F. Wolfgram, *J. Neurochem.* 13 (1966) 461–470.
[19] M. Arquini, J. Roder, L. S. Chia, J. Down, D. Wilkinson, H. Bayley, P. Braun, R. Dunn, *Proc. Natl. Acad. Sci. USA* 84 (1987) 600–604.
[20] W. T. Norton, S. E., *J. Neurochem.* 21 (1973) 759–773.
[21] M. V. Norgard, M. J. Tocci, J. J. Monahan, *J. Biol. Chem.* 255 (1980) 7665–7672.
[22] U. Gubler, B. J. Hoffman, *Gene* 25 (1983) 263–269.
[23] M. Schaich, R.-M. Budzinski, W. Stoffel, *Biol. Chem. Hoppe-Seyler* 367 (1986) 825–834.
[24] J. McLauchlan, D. Gaffney, J. L. Whitton, J. B. Clements, *Nucleic Acids Res.* 13 (1985) 1347–1368.
[25] H.-J. Diehl, M. Schaich, R.-M. Budzinski, W. Stoffel, *Proc. Natl. Acad. Sci. USA* 83 (1986) 9807–9811.
[26] E. J. Chen, P. H. Seeburg, *DNA* 4 (1985) 165–170.
[27] P. Heinrich: *Guidelines for Quick and Simple Plasmid Sequencing*, Boehringer Mannheim GmbH, Mannheim 1986.
[28] A. Dautigny, P. M. Alliel, L. d'Auriol, D. Pham-Dinh, J. L. Nussbaum, F. Galibert, P. Jollès, *FEBS Lett.* 188 (1985) 33–36.
[29] R. J. Milner, C. Lai, K. A. Nave, D. Lenoir, J. Ogata, J. G. Sutcliffe, *Cell* 42 (1985) 931–939.
[30] R. Breathnach, P. A. Chambon, *Annu. Rev. Biochem.* 50 (1981) 349–383.
[31] W. Gilbert, *Science* 228 (1985) 823–824.
[32] T. C. Südhof, J. L. Goldstein, M. L. Brown, D. H. Russell, *Science* 228 (1985) 815–822.
[33] D. Morello, A. Dautigny, D. Pham-Dinh, P. Jollès, *EMBO J.* 5 (1986) 3489–3493.
[34] L. D. Hudson, J. A. Bendt, C. Puckett, C. A. Kozak, R. A. Lazzarini, *Proc. Natl. Acad. Sci. USA* 84 (1987) 1454–1458.
[35] F. A. Ruddle, *Nature* 242 (1971) 165–169.
[36] H. F. Willard, J. R. Riordan, *Science* 230 (1985) 940–942.
[37] A. Dautigny, M. G. Mattei, D. Morello, P. M. Alliel, D. Pham-Dinh, L. Amar, D. Arnaud, D. Simon, J. F. Mattei, J. L. Guenet, P. Jollès, P. Avner, *Nature* 321 (1986) 867–869.
[38] P. R. Dunkley, P. R. Carnegie, *Biochem. J.* 141 (1974) 243–255.
[39] F. de Ferra, H. Engh, L. Hudson, J. Kamholz, C. Puckett, S. Molineaux, R. A. Lazzarini, *Cell* 43 (1985) 721–727.
[40] R. E. Mårtensson, G. E. Deibler, M. W. Kies, S. S. McKnally, R. Shapira, R. F. Kibler, *Biochim. Biophys. Acta* 263 (1972) 193–203.
[41] C. W. Campagnoni, G. D. Carey, A. T. Campagnoni, *Arch. Biochem. Biophys.* 190 (1978) 118–125.
[42] J. H. Carson, M. L. Nielson, E. Barbarese, *Dev. Biol.* 96 (1983) 485–492.
[43] A. Roach, N. Takahashi, D. Pravtcheva, F. Ruddle, L. Hood, *Cell* 42 (1985) 149–155.
[44] R. Streicher, W. Stoffel, *Biol. Chem. Hoppe-Seyler* 370 (1989) 503–510.
[45] D. S. Falconer, *Nature* 169 (1952) 664–665.
[46] M. F. Lyon, *Nature* 190 (1961) 372–373.
[47] S. M. Gartler, A. D. Riggs, *Annu. Rev. Genet.* 17 (1983) 155–190.
[48] A. L. Kerner, J. H. Carson, *J. Neurochem.* 43 (1984) 1706–1715.
[49] B. J. A. Sorg, D. Agrawal, H. C. Agrawal, A. T. Campagnoni, *J. Neurochem.* 46 (1986) 379–387.
[50] L. A. Nave, C. Kai, F. E. Bloom, R. J. Milner, *Proc. Natl. Acad. Sci. USA* 84 (1986) 1454–1458.
[51] M. V. Gardiner, W. B. Macklin, A. J. Diniak, P. L. Deininger, *Mol. Cell. Biol.* 6 (1986) 3755–3762.
[52] A. Meier, A. D. MacPike, *Exp. Brain Res.* 10 (1970) 512–528.
[53] S. Billings-Gagliardi, L. H. Adcock, M. K. Wolf, *Brain Res.* 194 (1980) 325–328.
[54] K. Yanagisawa, I. D. Duncan, J. P. Hammang, R. H. Quarles, *J. Neurochem.* 47 (1986) 1901–1907.
[55] D. Boison, W. Stoffel, *EMBO J.* 8 (1989) 3295–3302.
[56] D. F. Saxe, N. Takahashi, L. Hood, M. I. Simon, *Cytogenet. Cell. Genet.* 39 (1985) 246–249.

- [57] P. S. Sparkes, T. Mohandas, C. Heiman, H. J. Roth, I. Klissak, A. T. Campagnoni, *Hum. Genet.* 75 (1987) 147–150.
- [58] J. M. Matthieu, J. M. Roach, F. X. Omlin, I. Rauboldt, G. Almanzan, P. E. Braun, *J. Cell. Biol.* 103 (1986) 2673–2682.
- [59] C. Readhead, B. Popko, N. Takahashi, H. D. Shine, R. Saavedra, R. L. Sidman, L. Hood, *Cell* 48 (1987) 703–712.
- [60] B. Popko, C. Puckett, E. Lai, H. D. Shine, C. Readhead, N. Takahashi, S. W. Hunt, R. L. Sidman, L. Hood, *Cell* 48 (1987) 713–721.
- [61] E. L. Hogan, S. Greenfield in P. Morell (Ed.): *Myelin*, Plenum Press, New York 1984, pp. 489–534.
- [62] G. Neuhäuser in P. J. Vinken, C. W. Bryott (Eds.): *Handbook of Clinical Neurology*, North Holland, Amsterdam 1979, pp. 498–500.
- [63] N. Igahashi, H. Schaumburg, J. Power, Y. Kishimoto, E. Kolodemy, K. Suzuki, *J. Neurochem.* 26 (1976) 851–860.
- [64] J. Boué, I. Oberlé, R. Heilig, J. L. Mandel, A. Moser, W. Larsen, Y. Dumez, A. Boué, *Hum. Genet.* 69 (1985) 272–274.
- [65] I. Oberlé, D. Drayna, G. Camerino, R. White, J. L. Mandel, *Proc. Natl. Acad. Sci. USA* 82 (1985) 2824–2828.
- [66] F. Seitelberger in P. J. Vinken, C. W. Bryott (Eds.): *Handbook of Clinical Neurology*, North Holland, Amsterdam 1979, pp. 150–202.
- [67] A. H. Koeppen, N. A. Ronca, E. A. Greenfield, M. B. Hans, *Ann. Neurol.* 21 (1987) 159–170.
- [68] E. P. Reddy, M. Sandberg-Wollheim, R. V. Mettus, P. E. Ray, E. De Freitas, H. Koprowski, *Science* 243 (1989) 529.
- [69] S. Gencic, L. D. Hudson, *J. Neurosci.* 10 (1990) 117–124.
- [70] W. Stoffel, T. Weimbs, T. Dick, E. Boltshauser, unpublished.
- [71] J. A. Trofatter, S. R. Dlouky, W. De Myer, P. M. Conneally, M. E. Hodes, *Proc. Natl. Acad. Sci. (USA)* 86 (1989) 9427–9430.
- [72] L. D. Hudson, C. Puckett, J. Berndt, J. Chan, S. Gencic, *Proc. Natl. Acad. Sci. (USA)* 86 (1989) 8128–8131.
- [73] S. Gencic, D. Abuelo, M. Ambler, L. D. Hudson, *Am. J. Hum. Genet.* 45 (1989) 435–443.
-